Received: 28 February 2021 | Revised: 4 June 2021 | Accepted: 22 June 2021

IET Microwaves, Antennas & Propagation

DOI: 10.1049/mia2.12176

The Institution of Engineering and Technology WILEY

ORIGINAL RESEARCH PAPER

Integral transforms and the regularisation method in the time-domain excitation of open PEC slotted cone scatterers

Volodymyr O. Doroshenko | **Nadiia P. Stognii**

Department of Higher Mathematics, School of Information and Analytical Technologies and Management, Kharkiv National University of Radio Electronics, Kharkiv, Ukraine

Correspondence

Volodymyr O. Doroshenko, Department of Higher Mathematics, School of Information and Analytical Technologies and Management, Kharkiv National University of Radio Electronics, Nauky Ave., 14, Kharkiv 61166, Ukraine.

Email: volodymyr.doroshenko@nure.ua

Abstract

An initial-boundary value problem for the transient electromagnetic field in the presence of a complicated-shape scatterer is studied. The considered biconical zero-thickness and perfectly conducting surface with periodic longitudinal slots has many special cases, each of which is of separate practical interest. A new analytical-numerical technique is presented that is based on the Mehler–Fock integral transform and the method of analytical regularisation. The source of excitation of the slotted bicone is a radial electric dipole with an arbitrary time dependence on the field. The proposed method makes it possible to obtain an analytical and numerical solution of the problem to carry out a qualitative and numerical analysis, and to study the characteristic features of the main scattering. Due to the use of the method, the initial-boundary value problem is reduced to a Fredholm type of the second kind system of linear algebraic equations (SLAE-2). The dependences of the condition number on the problem parameters and the estimation of the SLAE-2 convergence with larger truncation orders are given. The far-field radiation patterns are plotted for various values of the problem parameters, the behaviour of the near field at the apex of the slotted cone is studied, and the regime of the slot wave propagation is analysed.

1 | INTRODUCTION

One of the urgent problems of the modern antenna technology and radar is the design and sophistication of broadband and ultra-wideband radar and other microwave systems with controlled patterns and polarisation of radiation. Two necessary conditions for practical, frequency-independent antennas are formulated in [1]: the angle principle and the truncation principle. The angle principle is based on the frequency independence of antennas if they are entirely defined by angle values. This is undoubted as, for the infinite frequency region of operation (bandwidth) the antenna geometry should be infinite. For a practical antenna (one of finite size) to achieve the frequency independence, the truncation principle must be satisfied—thus, the antenna must consist of 'active regions'. An active region corresponds to the antenna part that has the largest contribution to radiation at a particular frequency. Since the region moves along the antenna as the frequency is changed, the electric length and the performance of the antenna can remain uniform over a broadband. A practical biconical antenna has a geometry that differs from the ideal cone—for instance, at the feeding point. Besides, the reflections occur at the drive point and the end of the antenna, leading to radiated pulse distortions [1, 2]. Since in practice the objects of finite dimensions are used, a reasonable question arises about the limits of applicability of the results obtained in the study of the scattering from semi-infinite and infinite structures.

The above points indicate that antennas using metal cones, bicones, and angular sectors, the characteristic parameters of which are angular ones, have wideband and ultra-wideband properties. In article [3], it is shown that under the axial excitation of a linearly expanding perfectly electrically conducting (PEC) slot antenna (e.g. conical angular sector and angular cut in the PEC plane), if the source is near the apex of the cut, a travelling wave propagating along the slot is identified. The field of this wave determines the radiation pattern of the entire antenna, provided that the longitudinal length of the antenna

exceeds two wavelengths (in this case the end effects are negligible). To improve the radiation characteristics and eliminate the effect of the end of the antenna, in [2] the application of a resistive load to the surface of the conical PEC antenna is proposed, where the excitation source is at the apex of the cone.

Generally speaking, no universal full-wave method has been developed so far for studying the wave scattering from a semi-infinite PEC cone. Besides, the results of the analysis of the time-harmonic wave scattering from a semi-infinite impedance cone appeared relatively recently [4], and there is no similar full-wave analysis for a dielectric cone.

Research on the electromagnetic properties of various conical and biconical PEC scatterers, including angular sectors, has a long history [5–7] and, despite certain difficulties, continues attracting the attention of researchers [8–23]. Such objects are used as elements of aircraft fuselage and microstrip resonators [11, 24], array antennas, radiometers, surveillance systems [23, 25, 26] etc. The presence of surface singularities (tips, edges and slots) on such structures leads, for example, to the appearance of specific wave forms in the scattered fields. As it is known in ultra-wideband radar, the scattering of the probe pulse at certain individual local elements (scattering centres) largely represents the nature of the total diffraction field. Under certain conditions, the scattering from the edges and vortices of a complicated-shape object has the main contribution to the total and radar cross section [22]. Therefore, knowledge of the field behaviour at the vortices, spikes, and edges is important for the efficient computation of the fields scattered from the objects with surface singularities [11].

Evolution of the analysis of electromagnetic wave scattering from isotropic and open conical structures can be split into two lines of investigation depending on the time dependence of the physical process. The first line is connected with the time-harmonic scattering investigation. Here, one of the main methods has been the method of separation of variables. This method is also known as the method of eigenfunctions or the method of curvilinear coordinates and can be used for solving the scattering problems associated with the conical configurations of various geometries and surface properties [10, 27]. The use of [10] and the fact that one of the coordinate surfaces of the sphere-conical coordinate system is a plane angular sector enabled the authors of [15, 28] to derive the solution of the scattering from a PEC quarter plane for a semi-infinite plane angular sector. Among the advantages of the variables separation method, one can point to the convenience of the field analysis near the cone or plain sector apex and the derivation of an approximate solution in the case where the source is placed near the apex. The latter case is important for practical applications [3, 29]. The study of the field behaviour at the apex of a solid PEC cone was published in [11, 30]. Because of the slow convergence, the solution in the form of the eigenfunction series is not very suitable for numerical analysis in the high-frequency domain. The series representation as a contour integral allows to avoid such complications [31]. In contrast, the approach proposed in [14] allows one to obtain the field representations only in the high-frequency domain. It should be emphasised that the mathematical apparatus of the Kontorovich–Lebedev integral transform is a basic one in the full-wave study of the time-harmonic wave scattering from both infinite and finite conical configurations [31–33].

Empirical methods, which include the methods of physical optics [34], geometric theory of diffraction, and the physical theory of diffraction, were also used to study the scattering of waves from finite circular and elliptical cones [17, 18]. Such approaches are convenient when studying the scattering properties of complicated geometry objects. However, it is difficult to establish the limits of the applicability of the results obtained by these methods in the shadow and transition zones. This gap is partially bridged by the purely numerical methods [35, 36]. However, even the use of powerful computers does not remove certain problems here. The results obtained by empirical, approximate and numerical methods require validation by comparison with the known results obtained by the rigorous methods.

Rigorous numerical and numerical-analytical solution methods are the full-wave methods, which have complete mathematical grounding. They include the methods of expansion in terms of the eigenfunctions of the Helmholtz equation and integral transformations as well as the method of analytical regularisation (MAR) [33, 37–40]. In the past years, the MAR has been used to study a wide variety of time-harmonic scattering problems associated with PEC and imperfect scatterers [41–53]. The main merit of the MAR is that it ends up with the Fredholm second kind matrix equations, which have the convergence guaranteed by the Fredholm theorems. Thanks to the convergence, the accuracy of numerical solutions can be brought to machine precision. The MAR occupies a special place in the analysis of the scattering from the PEC conical and biconical scatterers, both infinite [31] and finite, including truncated cones [33, 39, 47]. In [54], the problem of elementary dipole excitation of an unbounded biconical PEC structure with longitudinal periodic slots was considered. As is known, the presence of slots on the surface of the cone contributes to the expansion of the frequency range of the corresponding realistic antenna [1]. To solve this problem, the authors of [54] used the Kontorovich–Lebedev integral transform in combination with the MAR, and an analysis of the influence of longitudinal slots on the near and far field was carried out.

The second line is related to the initial-boundary value problem investigations in the time-domain scattering [2, 20, 22, 35]. The authors of [22] analysed the features of the short pulse scattering by a finite solid PEC cone under the assumption that the scattered field can be represented as a superposition of pulses scattered from the resolved scattering centres. In [20], the travelling-wave approach was applied to obtain approximate analytical expressions for thin wire V-antennas excited by arbitrary time-dependent currents. A conical monopole antenna was considered in [2] as a pulse radiator. Here, the theoretical analysis of the antenna characteristics was based on the finite-difference time-domain (FDTD) method.

Representations for the time-dependent dyadic Green's functions for a PEC semi-infinite isotropic PEC cone were derived in [55]. The time-dependent response due to a point source in the presence of a semi-infinite cone was found through the Laplace inversion of the time-harmonic Green's time-dependent functions. This procedure can be used when inverting, for example, the potentials or components of a harmonic field, which are represented in the form of the Kontorovich–Lebedev integrals. The result of the inversion is a rigorous solution to the corresponding initial-boundary value problem for a cone or a bicone as well as for their particular cases. The unbounded biconical PEC structure with periodic slots, considered in [54], has a number of important special cases that are interesting both for the antenna theory and for practical applications. Among them, there are the models of objects of natural origin, conical and biconical slotted antennas and reflectors [2, 3, 7, 8, 12, 16, 20, 22], plane linearly tapered and butterfly type slot antennas [23, 25, 26], and conical slotted antennas located over the plane underlying surface [21].

As we will show in this work, due to the use of the inversion procedure, the solution of the boundary value problem for the biconical structure is transformed into the solution of the initial-boundary value problem, while the apparatus of the integral transformations of Kontorovich–Lebedev for the boundary problem is transformed into the apparatus of the integral Mehler–Fock transformations [56, 57] for the initial-boundary value problem. Due to this, the solution of the initial-boundary value problem can be derived immediately in the time domain using the Mehler–Fock integral transforms. In this connection, a rigorous analytical-numerical method based on the use of the Mehler–Fock integral transformations in combination with the MAR has been built and applied for the first time to study initial-boundary value problems associated with slotted conical geometry. The use of the latter makes it possible to obtain both an asymptotic analytical solution to the problem of an open conical structure excitation in the time domain and to carry out a numerical analysis of the scattering characteristics.

The rest of the study is arranged as follows: The statement of the problem and the motivation behind using the Mehler–Fock integral transform are given in Section 2. Approximations for the field in the case of a bicone with longitudinal slots are obtained in Section 3. The dual series equations are converted to a Fredholm second-kind infinite matrix equation and the field behaviour is analysed at the single slotted cone tip in Section 4. Section 5 presents the far-field patterns. Conclusions are given in Section 6.

2 | PROBLEM STATEMENT. THE MEHLER–FOCK INTEGRAL TRANSFORMS IN INITIAL-BOUNDARY VALUE ELECTROMAGNETIC PROBLEMS

Consider the wave scattering problem for a zero-thickness PEC biconical structure, $\Sigma = \Sigma_1 \cup \Sigma_2$, excited by elementary dipoles (see Figure 1). This conical structure consists of two

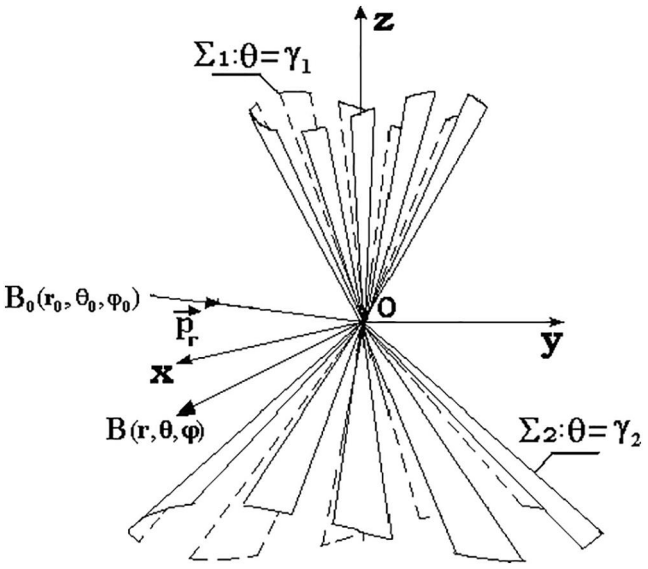

FIGURE 1 Geometry of the slotted biconical surface excited by elementary dipole

semi-infinite circular cones with a common axis and apex (centre of the surface Σ) denoted as point O. The cones Σ_1 and Σ_2 have equal number of periodic longitudinal slots, N. The aperture angle of the Σ_j-th cone ($j = 1, 2$) is $2\gamma_j$, the angular slot width is d_j, and the period is $l = 2\pi/N$. The value of the slot width (angular size) is equal to the value of the dihedral angle formed by the planes drawn through the axis of the cone and the edges of the strips.

The spherical coordinate system r, θ, φ is considered. Each of the cones Σ_j is defined by the equation $\theta = \gamma_j$ in this coordinate system. We will suppose that the $\varphi = 0$ plane cuts through one of the Σ_1 cone slot axes and the slot axes for the cones Σ_1 and Σ_2 do not match.

The given current source is either an electric, $\chi = 1$, or a magnetic, $\chi = 2$, elementary radial dipole with the moment

$$\vec{P}_r^{(\chi)}(\vec{r}, t) = \vec{M}^{(\chi)} \delta(\vec{r} - \vec{r}_0) f(t - t_0), \tag{1}$$

where point B_0 with coordinates $\vec{r}_0$ is the source point, $\delta(\vec{r} - \vec{r}_0)$ is a delta-function, and the $f(t - t_0)$ function defines the source field time variation so that $f(t - t_0) \equiv 0$, if $t < t_0$ (i.e. the source turns on when $t = t_0$). The conical structure and the source are placed in a homogeneous, isotropic stationary medium with permittivity ε and permeability μ. The task is to find the electromagnetic field $\vec{E}(\vec{r}, t)$, $\vec{H}(\vec{r}, t)$ in the presence of the conical structure and the source. This field should satisfy, at each moment of time, the following equations and conditions:

1) Maxwell equations;
2) Initial condition;

$$\vec{E} \equiv 0 \equiv \vec{H}, \text{if } t \le t_0 \tag{2}$$

3) Boundary condition on the conical surface Σ,

$$\vec{n} \times \vec{E}\Big|_{\Sigma} = 0, \tag{3}$$

where $\vec{n}$ is the unit normal to the surface Σ;
4) Local energy finiteness condition and
5) Condition at infinity.

The conditions (2)–(5) guarantee the uniqueness of the solution of the stated electromagnetic problem [4]. The field to be found can be presented as a sum,

$$\vec{E}(\vec{r},t) = \vec{E}_0(\vec{r},t) + \vec{E}_1(\vec{r},t), \tag{4}$$

$$\vec{H}(\vec{r},t) = \vec{H}_0(\vec{r},t) + \vec{H}_1(\vec{r},t), \tag{5}$$

where $\vec{E}_0(\vec{r},t)$ and $\vec{H}_0(\vec{r},t)$ correspond to the source field, while $\vec{E}_1(\vec{r},t)$ and $\vec{H}_1(\vec{r},t)$ characterise the field scattered from the conical surface.

It is convenient to express the electromagnetic field components via the electric $v^{(1)}$ (or magnetic $v^{(2)}$) Debye potential that satisfies the wave equation, initial conditions, boundary conditions, and the condition of the local energy finiteness.

The Debye potential $v^{(\chi)}(\vec{r},t)$ can be presented in the following form:

$$v^{(\chi)}(\vec{r},t) = v_0^{(\chi)}(\vec{r},t) + v_1^{(\chi)}(\vec{r},t), \tag{6}$$

where

$$v_0^{(\chi)} = -\frac{M_r^{(\chi)}}{4\pi r_0 \varepsilon^{2-\chi}\mu^{\chi-1}} \frac{1}{R} f\left(t - t_0 - \frac{1}{a}R\right)\eta\left(t - t_0 - \frac{1}{a}R\right) \tag{7}$$

is the potential corresponding to the source field, $v_1^{(\chi)}(\vec{r},t)$ is an unknown Debye's potential that corresponds to the scattered field, $\eta(\xi)$ is the Heaviside function and $R = \left|\vec{r} - \vec{r}_0\right|$.

We will use the Green's function method [4] and therefore define the Debye potential $v^{(\chi)}(\vec{r},t)$ according to the expression,

$$v^{(\chi)}(\vec{r},t) = \frac{M_r^{(\chi)}}{r_0 \varepsilon^{2-\chi}\mu^{\chi-1}} \int_0^{t-t_0} G^{(\chi)}(\vec{r} - \vec{r}_0, z) f(t - t_0 - z)dz, \tag{8}$$

where $G^{(\chi)}(\vec{r},t)$ is the Green's function of the considered initial-boundary value problem that satisfies the following conditions [4]:

1) Wave equation

$$\left(\Delta - \frac{1}{a^2}\frac{\partial^2}{\partial t^2}\right) G^{(\chi)}(\vec{r},t) = -\delta(\vec{r} - \vec{r}_0)\delta(t - t_0), \vec{r} \notin \Sigma; \tag{9}$$

where $\varepsilon\mu = a^{-2}$,

2) Initial condition

$$G^{(\chi)} \equiv 0 \equiv \frac{\partial G^{(\chi)}}{\partial t}, t \le t_0; \tag{10}$$

3) Boundary condition

$$\frac{\partial^{\chi-1}}{\partial n^{\chi-1}}\left(\frac{\partial G^{(\chi)}}{\partial t}\right)\Big|_{\Sigma} = 0, t \ge t_0, \tag{11}$$

$\vec{n}$ is the unit normal vector to the surface Σ.

4) Condition of the local energy finiteness

$$\iiint_V \left(\left|\frac{\partial G^{(\chi)}}{\partial t}\right|^2 + |\nabla G^{(\chi)}|^2\right) dV < \infty, \tag{12}$$

5) Condition at infinity

According to (6), the function $G^{(\chi)}(\vec{r},t)$ can be decomposed as follows:

$$G^{(\chi)}(\vec{r},t) = G_0(\vec{r},t) + G_1^{(\chi)}(\vec{r},t), \tag{13}$$

where $G_0(\vec{r},t)$ is the Green's function of the free space,

$$G_0(\vec{r},t) = \frac{\delta[t - t_0 - R/a]}{4\pi R}. \tag{14}$$

Thus, the solution of the electromagnetic scattering problem formulated above reduces to finding the transient Green's function $G_1^{(\chi)}(\vec{r},t)$ that corresponds to the field scattered from the slotted conical structure Σ.

The Green's function $G^{(\chi)}(\vec{r},t)$ can be transformed into the Laplace transform domain using the standard definition [4],

$$\tilde{G}^{s,(\chi)} = \tilde{G}^{s,(\chi)}(\vec{r}) = \int_0^{+\infty} G^{(\chi)}(\vec{r},t)e^{-st}dt, \operatorname{Re} s > 0. \tag{15}$$

Now, one should find function $\tilde{G}^{s,(1)}$ that satisfies

1) Inhomogeneous Helmholtz equation

$$\left(\Delta - q^2\right)\tilde{G}^{s,(\chi)}(\vec{r}) = -e^{-st_0}\delta\left(\vec{r} - \vec{r}_0\right), \vec{r} \notin \Sigma_0, q = s/a, \tag{16}$$

2) Boundary condition

$$\frac{\partial^{\chi-1}}{\partial n^{\chi-1}}\tilde{G}^{s,(\chi)}\Big|_{\Sigma} = 0; \tag{17}$$

3) Condition of local power finiteness

4) Condition at infinity

At first, we set $q > 0$ for definiteness (later, we will make analytical continuation in q into the complex half-plane $\mathrm{Re}\, q > 0 (\mathrm{Re}\, s > 0)$). Taking into account the uniqueness of the solution of the stated problem and the properties of the Laplace transform, we can conclude that the boundary value problem for the function $\tilde{G}^{s,(\chi)}$ has a unique solution as well. This function $\tilde{G}^{s,(\chi)}$ satisfies the Helmholtz equation off the slotted cone structure Σ and the source point.

According to Equations (10), (11) and (13), function $G^{s,(1)}$ should have the following form:

$$\tilde{G}^{s,(\chi)}(\vec{r}) = G_0^s(\vec{r}) + \tilde{G}_1^{s,(\chi)}(\vec{r}), \tag{18}$$

$$G_0^s(\vec{r}) = e^{-st_0}\frac{e^{-qR}}{4\pi R}. \tag{19}$$

Function $G_0^s(\vec{r})$ (13) can be presented in the Kontorovich–Lebedev integral form as follows [22, 23]:

$$G_0^s(\vec{r}) = \frac{2}{\pi^2}\int_0^{+\infty} \tau \mathrm{sh}\pi\tau \hat{G}_0^s \frac{K_{i\tau}(qr)}{\sqrt{r}} d\tau, \tag{20}$$

$$\hat{G}_0^s = \sum_{m=-\infty}^{+\infty} a_{m\tau}^s U_{m,i\tau}^{(0)} e^{im\varphi}, \tag{21}$$

$$U_{m,i\tau}^{(0)}(\theta,\theta_0) = \begin{cases} P_{-1/2+i\tau}^m(\cos\theta) P_{-1/2+i\tau}^m(-\cos\theta_0), \theta < \theta_0, \\ P_{-1/2+i\tau}^m(-\cos\theta) P_{-1/2+i\tau}^m(\cos\theta_0), \theta_0 < \theta, \end{cases} \tag{22}$$

$$a_{m\tau}^s = \frac{(-1)^m}{4\mathrm{ch}\pi\tau} e^{-im\varphi_0} e^{-st_0} \frac{K_{i\tau}(qr_0)}{\sqrt{r_0}} \frac{\Gamma\left(\frac{1}{2} - m + i\tau\right)}{\Gamma\left(\frac{1}{2} + m + i\tau\right)}, \tag{23}$$

where $K_{i\tau}(qr)$ is the McDonald function and $P_{-1/2+i\tau}^m(\cos\theta)$ is the associated Legendre function of the first kind. The unknown function $G_1^{s,(\chi)}(\vec{r})$ from (12) can be also sought in the form of the Kontorovich–Lebedev integral transforms,

$$G_1^{s,(\chi)}(\vec{r}) = \frac{2}{\pi^2}\int_0^{+\infty} \tau \mathrm{sh}\pi\tau \tilde{G}_1^{s,(\chi)} \frac{K_{i\tau}(qr)}{\sqrt{r}} d\tau, \tag{24}$$

$$\tilde{G}_1^{s,(\chi)} = \sum_{m=-\infty}^{+\infty} b_{m\tau}^s U_{m,i\tau}^{(\chi)}, \tag{25}$$

where $b_{m\tau}^s$ are known coefficients.

$$U_{m,i\tau}^{(\chi)} = \begin{cases} \sum\limits_{n=-\infty}^{+\infty} \alpha_{m,n}^{(\chi)} P_{-1/2+i\tau}^{m+nN}(\cos\theta) e^{i(m+nN)\varphi}, & 0 < \theta < \gamma_1, \\ \sum\limits_{n=-\infty}^{+\infty} \left[\beta_{m,n}^{(\chi)} P_{-1/2+i\tau}^{m+nN}(\cos\theta) + \xi_{m,n}^{(\chi)} P_{-1/2+i\tau}^{m+nN}(-\cos\theta)\right] e^{i(m+nN)\varphi}, & \gamma_1 < \theta < \gamma_2, \\ \sum\limits_{n=-\infty}^{+\infty} \eta_{m,n}^{(\chi)} P_{-1/2+i\tau}^{m+nN}(-\cos\theta) e^{i(m+nN)\varphi}, & \gamma_2 < \theta < \pi, \end{cases} \tag{26}$$

For finding the unknown coefficients $\alpha_{m,n}^{(\chi)}$ and $\eta_{m,n}^{(\chi)}$ ($\beta_{m,n}^{(\chi)}$ and $\xi_{m,n}^{(\chi)}$ are expressed via $\alpha_{m,n}^{(\chi)}$, $\eta_{m,n}^{(\chi)}$) we obtain the coupled dual series equations of the following form:

$$\sum_{n=-\infty}^{+\infty} z_{m,n}^{(\chi),\kappa} e^{inN\varphi} = g_{p,i\tau}^{(\chi),m}(\gamma_\kappa) e^{im_0 N\varphi}, \text{ at strips of } \Sigma_\kappa, \ \kappa = 1,2 \tag{27}$$

$$\begin{aligned} \sum_{n=-\infty}^{+\infty} & [N(n+\nu)]^{\tilde{\rho}(\chi)} \frac{|n|}{n}\left(1 - \varepsilon_{n,\kappa}^{(\chi)}\right) \\ & \left\{ z_{m,n}^{(\chi),1}\left[h_{i\tau}^{(\chi),(n+\nu)N}(\pi-\gamma_2, \pi-\gamma_1)\right]^{\kappa-1} \right. \\ & \left. - z_{m,n}^{(\chi),2}\left[h_{i\tau}^{(\chi),(n+\nu)N}(\gamma_1,\gamma_2)\right]^{2-\kappa} \right\} e^{inN\varphi} \\ & = 0, \text{ at slots of, } \Sigma_\kappa, \end{aligned} \tag{28}$$

$$\begin{aligned} z_{m,n}^{(\chi),\kappa} = {} & \delta_\kappa^1 \alpha_{m,n}^{(\chi)} \frac{d^{\chi-1}}{d\gamma_1^{\chi-1}} P_{-1/2+i\tau}^{(n+\nu)N}(\cos\gamma_1) \\ & + \delta_\kappa^2 \eta_{m,n}^{(\chi)} \frac{d^{\chi-1}}{d\gamma_2^{\chi-1}} P_{-1/2+i\tau}^{(n+\nu)N}(-\cos\gamma_2), \end{aligned}$$

$$[N(n+\nu)]^{\tilde{\rho}(\chi)}\frac{|n|}{n}\left(1-\varepsilon_{n,\kappa}^{(\chi)}\right)=\frac{(-1)^{(n+\nu)N+\chi-1}\mathrm{ch}\pi\tau}{\pi(\sin\gamma_\kappa)^{1-\tilde{\rho}(\chi)}}\frac{\Gamma(1/2+i\tau+(n+\nu)N)}{\Gamma(1/2+i\tau-(n+\nu)N)}$$
$$\times\frac{1}{\frac{d^{\chi-1}}{d\gamma_\kappa^{\chi-1}}P_{-1/2+i\tau}^{(n+\nu)N}(\cos\gamma_\kappa)\frac{d^{\chi-1}}{d\gamma_\kappa^{\chi-1}}P_{-1/2+i\tau}^{(n+\nu)N}(-\cos\gamma_\kappa)}\frac{1}{1-\hat{C}_{i\tau}^{(\chi),(n+\nu)N}(\gamma_1,\gamma_2)}, \tag{29}$$

$$\hat{C}_{i\tau}^{(\chi),m+nN}(\gamma_\kappa,\gamma_j)=\frac{\frac{d^{\chi-1}}{d\gamma_\kappa^{\chi-1}}P_{-1/2+i\tau}^{m+nN}(\cos\gamma_\kappa)}{\frac{d^{\chi-1}}{d\gamma_\kappa^{\chi-1}}P_{-1/2+i\tau}^{m+nN}(-\cos\gamma_\kappa)}\frac{\frac{d^{\chi-1}}{d\gamma_j^{\chi-1}}P_{-1/2+i\tau}^{m+nN}(-\cos\gamma_j)}{\frac{d^{\chi-1}}{d\gamma_j^{\chi-1}}P_{-1/2+i\tau}^{m+nN}(\cos\gamma_j)}, \tag{30}$$

$$h_{i\tau}^{(\chi),m}(x,y)=\frac{\frac{d^{\chi-1}}{dx^{\chi-1}}P_{-1/2+i\tau}^{m}(\cos x)}{\frac{d^{\chi-1}}{dy^{\chi-1}}P_{-1/2+i\tau}^{m}(\cos y)},$$
$$g_{p,i\tau}^{(\chi),m}(\theta)=\frac{1}{\hat{b}_{m\tau}^{(\chi),p}(\gamma_p,\theta_0)}\frac{d^{\chi-1}}{d\theta^{\chi-1}}U_{m\tau}^{(0)}(\theta,\theta_0), \tag{31}$$

where $m/N=m_0+\nu$, m_0 is the closest integer number to m/N, $-1/2\le\nu<1/2$,

$$\delta_n^m=\begin{cases}1, n=m,\\ 0, n\ne m.\end{cases} \tag{32}$$

The condition of local energy finiteness provides the limitation according to which the unknown coefficients $\tilde{z}_{m,n}^{(\chi),j}$ should belong to the Hilbert space ℓ^2 of infinite sequences with the scalar product,

$$X\cdot Y=\sum_{n=-\infty}^{+\infty}(1+|n|)^{\tilde{\rho}(\chi)}X_n\bar{Y}_n, \tag{33}$$

where the line above the symbol means conjugation. Also,

$$\sum_{n=-\infty}^{+\infty}(1+|n|)^{\rho(\chi)}\left|\tilde{z}_{m,n}^{(\chi),j}\right|^2<+\infty. \tag{34}$$

As the right-hand part of Equation (27) does not depend on parameter q and on the $N(n+\nu)\frac{|n|}{n}(1-\varepsilon_{m,n}^{(\chi)})$ coefficients that are defined in Equation (29) and included in the left hand part of Equation (28), the coefficients $z_{m,n}^{(\chi),\kappa}$ and the function $U_{m,i\tau}^{(\chi)}$ (26) are independent of parameter q.

Using the approach given in [23], the Green's function $G_1^{(\chi)}(\vec{r},t)$ (13) of the boundary value problem for the considered cone with longitudinal slots can be uniquely presented in the form of the integral,

$$G_1^{(\chi)}(\vec{r},t)=\int_0^{+\infty}\tau\mathrm{th}\pi\tau\hat{G}_1^{(\chi)}P_{-1/2+i\tau}[\mathrm{ch}b(t-t_0)]d\tau, \tag{35}$$

where

$$\hat{G}_1^{(\chi)}=-\frac{1}{r}\eta\left(t-t_0-\frac{r+r_0}{a}\right)$$
$$\sum_{m=-\infty}^{+\infty}\hat{a}_{m\tau}U_{m,i\tau}^{(\chi)}P_{-1/2+i\tau}^{m}(-\cos\theta_0)P_{-1/2+i\tau}^{m}(\cos\gamma), \tag{36}$$

$$\hat{a}_{m\tau}=\frac{1}{4\pi r_0}(-1)^m e^{-im\varphi_0}\frac{\Gamma\left(\frac{1}{2}-m+i\tau\right)}{\Gamma\left(\frac{1}{2}+m+i\tau\right)}, \tag{37}$$

$$\mathrm{ch}b(z)=\frac{a^2z^2-r^2-r_0^2}{2rr_0}, b\in[0,+\infty), \tag{38}$$

The main idea behind this approach is to use the following representation:

$$K_{i\tau}(qr_0)K_{i\tau}(qr)=\frac{1}{2}\int_0^{+\infty}K_0\left(q\sqrt{r^2+r_0^2+2rr_0\mathrm{ch}\tilde{\mu}}\right)e^{i\tau\tilde{\mu}}d\tilde{\mu}, \tag{39}$$

$$K_0(q\widehat{\chi})=\int_{\widehat{\chi}/a}^{+\infty}\frac{e^{-s\alpha}}{\sqrt{v^2-\widehat{\chi}^2/a^2}}d\alpha. \tag{40}$$

The Green's function $G_0(\vec{r},t)$ can also be represented in a form similar to Equation (35) with the aid of the Mehler–Dirichlet integral transform, defined as follows:

$$\hat{F}(\tau)=\int_0^{+\infty}\mathrm{sh}bF(b)P_{-1/2+i\tau}(\mathrm{ch}b)db, b\in[0,+\infty), \tag{41}$$

$$F(b) = \int_0^{+\infty} \tau \mathrm{th}\pi\tau \hat{F}(\tau) P_{-1/2+i\tau}(\mathrm{ch}b) d\tau. \quad (42)$$

It should be noted that for inverting $G_1^{s,(\chi)}$ and representing $G^{(\chi)}(\vec{r},t)$ in the form of the Mehler–Fock integral transforms (41), (42) [22, 23], one should use formulas (39) and (40) each time. This procedure was used for the first time in [4, 24], where the Green's functions for the first and second boundary value problems of the wave equation for a PEC wedge and for a semi-infinite circular isotropic PEC cone were considered. In these works, where the Green's function representation was derived, it was necessary to perform the inversion procedure. In the stationary problem inversion, the kernel of the Kontorovich–Lebedev integral transform gets inverted. As a result, the $P_{-1/2+i\tau}(\mathrm{ch}b)$ as a kernel of the Mehler–Fock integral transform (41), (42) appears. Thus, the Mehler–Fock integral transform (41), (42) is a generalisation of the Kontorovich–Lebedev integral transforms,

$$\hat{g}(\tau) = \int_0^{+\infty} g(r) \frac{K_{i\tau}(qr)}{\sqrt{r}} dr, \quad (43)$$

$$g(r) = \frac{2}{\pi^2} \int_0^{+\infty} \tau \mathrm{sh}\pi\tau \hat{g}(\tau) \frac{K_{i\tau}(qr)}{\sqrt{r}} d\tau, \quad (44)$$

for the solution of the boundary value problems associated with wedges and isotropic cones in the time domain. It is also possible to extend the use of the Mehler–Fock transforms to the solution of the problems with open conical geometries, including conical structures with longitudinal slots. Thus, the use of the Mehler–Fock integral transforms (41), (42) makes it possible to obtain a solution without applying the procedure of inversion of the stationary problem solution.

Generally speaking, one can apply the approach presented above, provided that the field dependence on time (including harmonic one) is given.

Taking into account the representation (35) for the Green's function and (8), the Debye potential $v_1^{(\chi)}(\vec{r},t)$ from (6) can be written as follows:

$$v_1^{(\chi)}(\vec{r},t) = \frac{aM_r^{(\chi)}}{4\pi r r_0^2 e^{2-\chi} \mu^{\chi-1}} \eta\left(t - t_0 - \frac{r+r_0}{a}\right) \times \sum_{m=-\infty}^{+\infty} (-1)^m e^{-im\varphi_0} \int_0^{+\infty} \tau \mathrm{th}\pi\tau \frac{\Gamma(1/2-m+i\tau)}{\Gamma(1/2+m+i\tau)} \hat{b}_{m\tau}^{(\chi)} U_{m,i\tau}^{(\chi)}(\theta,\varphi) \Phi_{i\tau}(t,r) d\tau, \quad (45)$$

$$\Phi_{i\tau}(t,r) = \int_{\frac{r+r_0}{a}}^{t-t_0} f(t-t_0-z) P_{-1/2+i\tau}(\mathrm{ch}b(z)) dz, \quad (46)$$

where $\hat{b}_{m\tau}^{(\chi)}$ are known coefficients.

The function $U_{m\tau}^{(\chi)}(\theta,\varphi)$ in Equations (26) and (45) depends on the conical structure geometry, and the function $\Phi_{i\tau}(t,r)$ (46) is completely defined by the source type.

3 | REPRESENTATIONS FOR THE DEBYE POTENTIALS AND FIELD APPROXIMATIONS

By using the relations between the Legendre functions of the first $P_{-i/2+i\tau}(u)$ and second $Q_{-i/2+i\tau}(u)$kind [27], the potential $v_1^{(\chi)}(\vec{r},t)$ (45) can be presented as

$$v_1^{(\chi)}(\vec{r},t) = \frac{ai\hat{p}_\chi}{4\pi^2 r r_0^2} \eta\left(t - t_0 - \frac{r+r_0}{a}\right) \sum_{m=-\infty}^{+\infty} (-1)^m e^{-im\varphi_0} \times \int_0^{+\infty} \tau \mathrm{th}\pi\tau \frac{\Gamma(1/2-m+i\tau)}{\Gamma(1/2+m+i\tau)} \hat{b}_{m\tau}^{(\chi)} U_{m,i\tau}^{(\chi)}(\theta,\varphi) \left[\widehat{\Psi}_{i\tau}(t,r) - \widehat{\Psi}_{-i\tau}(t,r)\right] d\tau, \quad (47)$$

$$\widehat{\Psi}_{i\tau}(t,r) = \int_{\frac{r+r_0}{a}}^{t-t_0} f(t-t_0-z) Q_{-1/2+i\tau}(\mathrm{ch}b(z)) dz. \quad (48)$$

Suppose now that the source is located at the axis ($\theta_0 = \pi$) of the slotted conical structure. Then, the representation for (47) gets simpler,

$$v_1^{(\chi)}(\vec{r},t) = \frac{ai\hat{p}_\chi}{4\pi^2 r r_0^2} \eta\left(t - t_0 - \frac{r+r_0}{a}\right) \times \int_0^{+\infty} \tau \frac{d^{\chi-1}}{d\gamma_2^{\chi-1}} P_{-1/2+i\tau}(\cos\gamma_2) U_{0,i\tau}^{(\chi)}(\theta,\varphi) \left[\widehat{\Psi}_{i\tau}(t,r) - \widehat{\Psi}_{-i\tau}(t,r)\right] d\tau. \quad (49)$$

The integral representations (45), (47), (49) are convenient for the field analysis in the transition regions. In order to study the spatial field distribution in the case of close location of the source to the centre of the slotted conical structure ($r_0 \ll 1$) and

near the conical structure origin ($r << 1$), one should use the series representations for the potential $v_1^{(\chi)}(\vec{r},t)$ and the field components. To derive them, we represent $v_1^{(\chi)}(\vec{r},t)$ as follows:

$$v_1^{(\chi)}(\vec{r},t) = -\frac{ai\hat{p}_\chi}{4\pi^2 r r_0{}^2}\eta\left(t-t_0-\frac{r+r_0}{a}\right) \times \int_{-i\infty}^{+i\infty} \hat{\mu}\frac{d^{\chi-1}}{d\gamma_2^{\chi-1}}P_{-1/2+\hat{\mu}}(\cos\gamma_2)U_{0,\hat{\mu}}^{(\chi)}(\theta,\varphi)\widehat{\Psi}\hat{\mu}(t,r)d\hat{\mu}. \quad (50)$$

It should be noted that the function $U_{0,\hat{\mu}}^{(\chi)}(\theta,\varphi)$ has isolated singularity points that represent simple poles located on the $\mathrm{Re}\hat{\mu}$ axis in the complex plain of the complex variable $\hat{\mu}$. Therefore, this function can be represented in the form,

$$U_{0,\hat{\mu}}^{(\chi)}(\theta,\varphi) = \frac{\hat{g}_{\hat{\mu}}^{(\chi)}(\theta,\varphi)}{\hat{G}_{\hat{\mu}}^{(\chi)}}. \quad (51)$$

After the closure of the integration contour (50) in the right half plane ($\mathrm{Re}\,\hat{\mu} > 0$) of the complex plane of the variable $\hat{\mu}$ and the application of the residue theorem, we obtain the representations of the potential $v^{(\chi)}(\vec{r},t)$ for the full-field $\vec{E}$, $\vec{H}$ in the form of the residue series over the integrand poles,

$$v^{(\chi)}(\vec{r},t) = -\frac{a\hat{p}_\chi}{2\pi r r_0^2}\eta\left(t-t_0-\frac{r+r_0}{a}\right) \times \sum_{s=o}^{+\infty}\hat{\mu}_s^{(\chi)}\frac{\hat{g}_{\hat{\mu}}^{(\chi)}}{\frac{d}{d\hat{\mu}}\hat{G}_{\hat{\mu}}^{(\chi)}}\Big|_{\hat{\mu}=\hat{\mu}_s^{(\chi)}}\frac{d^{\chi-1}}{d\gamma_2^{\chi-1}}P_{-1/2+\hat{\mu}_s^{(\chi)}}(\cos\gamma_2)\widehat{\Psi}_{\hat{\mu}_s^{(\chi)}}(t,r), \quad (52)$$

where $\hat{\mu}_s^{(\chi)}$ are simple zeros of the function $\hat{G}\hat{\mu}^{(\chi)}$ involved into (51), that is,

$$\hat{G}_{\hat{\mu}}^{(\chi)}\big|_{\hat{\mu}=\hat{\mu}_s^{(\chi)}} = 0. \quad (53)$$

It follows from Equation (52) that in the case of the axially symmetric excitation ($\theta_0 = \pi$), the spatial spectrum of the considered initial-boundary value problem is a set of the roots in Equation (53). In this case, by the spectrum of eigenvalues, we mean the set of poles $\hat{\mu}_s^{(\chi)}$ of the integrand. As a result, we obtain a representation for the potential in the form of a series, each term of which is a solution of the wave equation. As the function $U_{m,i\tau}^{(\chi)}(\theta,\varphi)$ (26) depends on the considered conical geometry, the spatial spectrums of the initial-boundary problems for the corresponding particular conical structures depend on their parameters. The spectrum $\{\hat{\mu}_s^{(\chi)}(\gamma_2,d)\}_{s=0}^{+\infty}$ of the considered initial-boundary value problem is a discrete real-valued monotonously increasing sequence, the minimum element of which $\hat{\mu}_0^{(\chi)}$ is larger than 0.5.

The representation (52) can be used to solve the problem in the stabilised regime, that is $a(t-t_0) >> 1$ and $a(t-t_0) >> r^2 + r_0^2$, in the case of $f(t-t_0) = \delta(t-t_0)$. It should be noted that in order to study the field near the wave front, $a(t-t_0) = r + r_0$, the expressions (47)–(50), and (52) are impractical. The formulas for the wave front vicinity should be derived directly from Equation (45), which can be represented as follows:

$$v_1^{(\chi)}(\vec{r},t) = \frac{a\hat{p}_\chi}{4\pi r r_0{}^2}\eta\left(t-t_0-\frac{r+r_0}{a}\right) \times \sum_{m=-\infty}^{+\infty}(-1)^m e^{-im\varphi_0}\int_0^{+\infty}\tau\,\mathrm{th}\pi\tau\frac{\Gamma(1/2-m+i\tau)}{\Gamma(1/2+m+i\tau)} \hat{b}_{m\tau}^{(\chi)}U_{m,i\tau}^{(\chi)}(\theta,\varphi)P_{-1/2+i\tau}(\mathrm{ch}b(t-t_0))d\tau, \quad (54)$$

where $a(t-t_0) - r + r_0 << 1$ and

$$\mathrm{ch}b(t-t_0) - 1 = \frac{a^2(t-t_0)^2 - (r+r_0)^2}{2rr_0} << 1. \quad (55)$$

The asymptotic representation for $v_1^{(\chi)}(\vec{r},t)$ near the wave front is obtained as

$$v_1^{(\chi)}(\vec{r},t) = \frac{a\hat{p}_\chi}{4\pi r r_0{}^2}\eta\left(t-t_0-\frac{r+r_0}{a}\right) \times \left\{\sum_{m=-\infty}^{+\infty}(-1)^m e^{-im\varphi_0}\int_0^{+\infty}\tau\,\mathrm{th}\pi\tau\frac{\Gamma(1/2-m+i\tau)}{\Gamma(1/2+m+i\tau)}\hat{b}\{_{m\tau}^{(\chi)}U_{m,i\tau}^{(\chi)}d\tau - \frac{1}{2}\hat{\xi}\sum_{m=-\infty}^{+\infty}(-1)^m e^{-im\varphi_0}\int_0^{+\infty}\tau\left(\tau^2+\frac{1}{4}\right)\mathrm{th}\pi\tau\frac{\Gamma(1/2-m+i\tau)}{\Gamma(1/2+m+i\tau)}\hat{b}_{m\tau}^{(\chi)}U_{m,i\tau}^{(\chi)}(\theta,\varphi)d\tau\right\} + O(\hat{\xi}^2), \quad (56)$$

$$\hat{\xi} = \frac{a^2(t-t_0)^2 - (r+r_0)^2}{2rr_0} << 1. \quad (57)$$

In the case of the excitation by the elementary radial electric dipole ($\chi = 1$), the electric field components have the following form:

$$E_{\theta,1}=\frac{a\hat{p}_1}{4\pi r{r_0}^2}\eta\left(t-t_0-\frac{r+r_0}{a}\right)\times\sum_{m=-\infty}^{+\infty}(-1)^m e^{-im\varphi_0}\int_0^{+\infty}\tau\mathrm{th}\pi\tau\frac{\Gamma(1/2-m+i\tau)}{\Gamma(1/2+m+i\tau)}\hat{b}_{m\tau}^{(1)}\frac{\partial}{\partial\theta}U_{m,i\tau}^{(1)}(\theta,\varphi)\frac{\partial}{\partial r}\{r\Phi_{i\tau}(t,r)\}d\tau, \quad (58)$$

$$E_{\varphi,1}=\frac{a\hat{p}_1}{4\pi r{r_0}^2\sin\theta}\eta\left(t-t_0-\frac{r+r_0}{a}\right)\times\sum_{m=-\infty}^{+\infty}(-1)^m e^{-im\varphi_0}\int_0^{+\infty}\tau\mathrm{th}\pi\tau\frac{\Gamma(1/2-m+i\tau)}{\Gamma(1/2+m+i\tau)}\hat{b}_{m\tau}^{(1)}\frac{\partial}{\partial\varphi}U_{m,i\tau}^{(1)}(\theta,\varphi)\frac{\partial}{\partial r}\{r\Phi_{i\tau}(t,r)\}d\tau. \quad (59)$$

Assuming that the source is located at the cone axis ($\theta_0=\pi, m=0$), the components $E_{\theta,1}$, $E_{\varphi,1}$ of the scattered electric field can be represented in the form of a series over the integrand poles of the right hand part of Equation (58),

$$E_{\theta,1}=-\frac{a\hat{p}_1}{2\pi r^2{r_0}^2}\eta\left(t-t_0-\frac{r+r_0}{a}\right)\sum_{s=o}^{+\infty}\hat{\hat{\mu}}_s^{(1)}\times\frac{\frac{\partial}{\partial\theta}\hat{g}_{\hat{\mu}}^{(1)}}{\frac{d}{d\hat{\mu}}\hat{G}_{\hat{\mu}^{(1)}}}\Big|_{\hat{\mu}=\hat{\hat{\mu}}_s^{(1)}}P_{-1/2+\hat{\hat{\mu}}_s^{(1)}}(\cos\gamma_2)\frac{\partial}{\partial r}\left[\widehat{\Psi}_{\hat{\hat{\mu}}_s^{(1)}}(t,r)\right], \quad (60)$$

$$E_{\varphi,1}=-\frac{a\hat{p}_1}{2\pi r^2{r_0}^2\sin\theta}\eta\left(t-t_0-\frac{r+r_0}{a}\right)\sum_{s=o}^{+\infty}\hat{\hat{\mu}}_s^{(1)}\times\frac{\frac{\partial}{\partial\varphi}\hat{g}_{\hat{\mu}}^{(1)}}{\frac{d}{d\hat{\mu}}\hat{G}_{\hat{\mu}}^{(1)}}\Big|_{\hat{\mu}=\hat{\hat{\mu}}_s^{(1)}}P_{-1/2+\hat{\hat{\mu}}_s^{(1)}}(\cos\gamma_2)\frac{\partial}{\partial r}\left[\widehat{\Psi}_{\hat{\hat{\mu}}_s^{(1)}}(t,r)\right]. \quad (61)$$

If, additionally, the source is located near the centre ($r_0<<1$, $r_0<r$) of the surface, the dominant term defining the field in each of the aforementioned cases, where $\mathrm{ch}b>>1$, can be selected from the series to study the field behaviour near the centre. In this case, Equation (60) can be transformed as follows:

$$h(z,r,r_0)=\frac{a^2z^2+r^2-r_0^2}{\sqrt{a^2z^2-(r+r_0)^2}\sqrt{a^2z^2-(r-r_0)^2}}, \quad (63)$$

provided that $t-t_0>(r+r_0)/a$.

The summation in Equation (62) is made over the numbers of the spectral values, the minimum of which, $\hat{\hat{\mu}}_0^{(1)}$, is larger than 0.5 for all conical structure parameters. One of the spatial spectrum features is the fact that its neighbour values differ from each other almost by the unit. This means that if $r<<1$ or $r_0<<1$, then the most significant contribution to the series comes from the first term, corresponding to the minimum spectral value $\hat{\hat{\mu}}_0^{(1)}$. The amplitude of this term is large if $r<<1$ or $r_0<<1$, while the absolute value of the second series term corresponding to $\hat{\hat{\mu}}_1^{(1)}>3/2$ is much smaller than the first one. The third series term is much smaller than the second, provided $r<<1$ or $r_0<<1$ etc. Thus, if the condition $r<<1$ or $r_0<<1$ is valid, it is enough to consider only the first term of the series (62) to obtain the approximate solution. In the particular case where $\chi=1$, the following approximation for $E_{\theta,1}$ is obtained from Equation (62):

$$E_{\theta,1}^{(0)}=-\frac{a\hat{p}_1}{2\sqrt{\pi}}\eta\left(t-t_0-\frac{r+r_0}{a}\right){r_0}^{-3/2+\hat{\hat{\mu}}_0^{(1)}}r^{-3/2+\hat{\hat{\mu}}_0^{(1)}}\times\frac{\Gamma\left(3/2+\hat{\hat{\mu}}_0^{(1)}\right)}{\Gamma\left(\hat{\hat{\mu}}_0^{(1)}\right)}P_{-1/2+\hat{\hat{\mu}}_0^{(1)}}(\cos\gamma_2)\times\frac{\frac{\partial}{\partial\theta}\hat{g}_{\hat{\mu}}^{(1)}(\theta,\varphi)}{\frac{d}{d\hat{\mu}}\hat{G}_{\hat{\mu}}^{(1)}}\Big|_{\hat{\mu}=\hat{\hat{\mu}}_0^{(1)}}\hat{F}_{\hat{\hat{\mu}}_0^{(1)}}^{(1)}(t;r,r_0), \quad (64)$$

$$\hat{F}_{\hat{\hat{\mu}}_0^{(1)}}^{(1)}(t;r,r_0)=\int_{\frac{r+r_0}{a}}^{t-t_0}\frac{f(t-t_0-z)}{(a^2z^2-r^2-r_0^2)^{\hat{\hat{\mu}}_0^{(1)}+1/2}}h(z,r,r_0)dz. \quad (65)$$

Here, the electromagnetic field near the centre of the conical surface behaves as follows:

$$\left|\vec{E}\right|\sim r^{-1+\alpha}$$

$$\left|\vec{H}\right|\sim r^{\alpha}, r<<1$$

$$E_{\theta,1}^{''}=-\frac{a\hat{p}_1}{2\sqrt{\pi}}\sum_{s=o}^{+\infty}(rr_0)^{-3/2+\hat{\hat{\mu}}_s^{(1)}}\frac{\Gamma\left(3/2+\hat{\hat{\mu}}_s^{(1)}\right)}{\Gamma\left(\hat{\hat{\mu}}_s^{(1)}\right)}\frac{\frac{\partial}{\partial\theta}\hat{g}_{\hat{\mu}}^{(1)}(\theta,\varphi)}{\frac{d}{d\hat{\mu}}\hat{G}_{\hat{\mu}}^{(1)}}\Big|_{\hat{\mu}=\hat{\hat{\mu}}_s^{(1)}}P_{-1/2+\hat{\hat{\mu}}_s^{(1)}}(\cos\gamma_2)\times\int_{\frac{r+r_0}{a}}^{t-t_0}\frac{f(t-t_0-z)}{(a^2z^2-r^2-r_0^2)^{\hat{\hat{\mu}}_s^{(1)}+1/2}}h(z,r,r_0)\left[1+O\left(\left(\frac{rr_0}{a^2z^2-r^2-r_0^2}\right)^2\right)\right]dz, \quad (62)$$

$$\alpha = -1/2 + \hat{\hat{\mu}}_0^{(1)}, \hat{\hat{\mu}}_0^{(1)} = \min_s \hat{\hat{\mu}}_s^{(1)}. \tag{66}$$

In the case of the δ-impulse, source $E_{\theta,1}^{(0)}$ (64) takes the form of

$$E_{\theta,1}^{(0)} = -\frac{a\hat{p}_1}{2\sqrt{\pi}}\eta\left(t - t_0 - \frac{r + r_0}{a}\right) r_0^{-3/2+\hat{\hat{\mu}}_0^{(1)}} r^{-3/2+\hat{\hat{\mu}}_0^{(1)}} \times \frac{\Gamma\left(3/2 + \hat{\hat{\mu}}_0^{(1)}\right)}{\Gamma\left(\hat{\hat{\mu}}_0^{(1)}\right)} P_{-1/2+\hat{\hat{\mu}}_0^{(1)}}(\cos\gamma_2) \times \frac{\frac{\partial}{\partial\theta}\hat{g}_{\hat{\mu}}^{(1)}(\theta,\varphi)}{\frac{d}{d\hat{\mu}}\hat{G}_{\hat{\mu}}^{(1)}}\Big|_{\hat{\mu}=\hat{\hat{\mu}}_0^{(1)}} \frac{h(t - t_0, r, r_0)}{\left(a^2(t - t_0)^2 - r^2 - r_0^2\right)^{\hat{\hat{\mu}}_0^{(1)}+1/2}}. \tag{67}$$

Provided that $a(t - t_0) >> 1$, that is, in the late-time regime, the expression for $E_{\theta,1}^{(0)}$ can be obtained from Equation (67) as

$$E_{\theta,1}^{(*)} = -\frac{a\hat{p}_1}{2\sqrt{\pi}} r_0^{-3/2+\hat{\hat{\mu}}_0^{(1)}} r^{-3/2+\hat{\hat{\mu}}_0^{(1)}} \times \frac{\left(\hat{\hat{\mu}}_0^{(1)} + 1/2\right)}{\frac{d}{d\hat{\mu}}\hat{G}_{\hat{\mu}}^{(1)}|_{\hat{\mu}=\hat{\hat{\mu}}_0^{(1)}}} \frac{\Gamma\left(\hat{\hat{\mu}}_0^{(1)} + 1/2\right)}{\Gamma\left(\hat{\hat{\mu}}_0^{(1)}\right)} P_{-1/2+\hat{\hat{\mu}}_0^{(1)}}(\cos\gamma_2) \times \frac{\frac{\partial}{\partial\theta}\hat{g}_{\hat{\mu}_0^{(1)}}^{(1)}(\theta,\varphi)}{\left(a(t - t_0)\right)^{2\hat{\hat{\mu}}_0^{(1)}+1}} \left[1 + O\left(a^{-2}(t - t_0)^{-2}\right)\right]. \tag{68}$$

4 | CONE WITH PERIODIC LONGITUDINAL SLOTS: THE REGULARISATION METHOD

Consider the problem of elementary dipole excitation for a single circular semi-infinite zero-thickness PEC cone $\Sigma_1 : \theta = \gamma,\ \gamma_1 = \gamma$, with N periodic longitudinal slots $(l = 2\pi/N)$ of the angular width d. In this case, the function $U_{m,i\tau}^{(\chi)}(\theta,\varphi)$ from the integral representation of the potential $v_1^{(\chi)}(\vec{r},t)$ (45) has the form,

$$U_{m,i\tau}^{(\chi)}(\theta,\varphi) = \sum_{n=-\infty}^{+\infty} x_{m,n+m_0}^{(\chi)} \frac{P_{-1/2+i\tau}^{m+nN}(\pm\cos\theta)}{\frac{d^{\chi-1}}{d\gamma_2^{\chi-1}}P_{-1/2+i\tau}^{m+nN}(\pm\cos\gamma)} e^{i(m+nN)\varphi}. \tag{69}$$

In Equation (33), the «+» sign in the Legendre functions corresponds to the $0 < \theta < \gamma$ region, and the «−» sign corresponds to the $\gamma < \theta < \pi$ region. The unknown coefficients $x_{m,n+m_0}^{(\chi)}$ satisfy the following dual series equations:

$$\sum_{n=-\infty}^{+\infty} x_{m,n}^{(\chi)} e^{inN\varphi} = e^{im_0N\varphi}, \text{ on strips}, \tag{70}$$

$$\sum_{n=-\infty}^{+\infty} [N(n+\nu)]^{\tilde{\rho}(\chi)}\frac{|n|}{n}\left(1 - \hat{\varepsilon}_n^{(\chi)}\right) x_{m,n}^{(\chi)} e^{inN\varphi} = 0, \text{ on slots}, \tag{71}$$

$$[N(n+\nu)]^{\tilde{\rho}(\chi)}\frac{|n|}{n}\left(1 - \hat{\varepsilon}_n^{(\chi)}\right) = \frac{(-1)^{(n+\nu)/N+\chi-1}\mathrm{ch}\pi\tau}{\pi(\sin\gamma)^{1-\tilde{\rho}(\chi)}} \frac{\Gamma(1/2 + i\tau + (n+\nu)N)}{\Gamma(1/2 + i\tau - (n+\nu)N)} \times \frac{1}{\frac{d^{\chi-1}}{d\gamma^{\chi-1}}P_{-1/2+i\tau}^{(n+\nu)N}(\cos\gamma)\frac{d^{\chi-1}}{d\gamma^{\chi-1}}P_{-1/2+i\tau}^{(n+\nu)N}(-\cos\gamma)}, \tag{72}$$

$$\hat{\varepsilon}_n^{(\chi)} = O\left(\frac{\sin^2\gamma}{N^2(n+\nu)^2}\right), N(n+\nu) >> 1. \tag{73}$$

The dual-series equations (70), (71) can be written in the operator form as

$$AY = B \tag{74}$$

where the operator A is a singular one; the singularity corresponds to the growth with $|n| \to \infty$ weight in the left-hand part of Equation (71).

Thus, in order to build a mathematically convergent numerical algorithm for the solution of Equation (74), a regularisation procedure of this equation must be developed.

The main idea behind this procedure is to present the operator A in Equation (74) as a sum of the singular operator A_0, which has a bounded inverse operator A_0^{-1} and an operator A_1, which is a compact operator in the Hilbert solutions' space ℓ^2,

$$A = A_0 + A_1. \tag{75}$$

Here, A_0 is the main part of A and A_1 is its regular part [37–40]. The form of operators A, A_0 and A_1 is defined by the dual series equations in each case. In the wave scattering problems associated with PEC zero-thickness strip gratings and open cylindrical and spherical screens, A_0 corresponds to the electrostatic part of the operator A, that is, $A = A_0$ if wavenumber $k = 0$.

After applying operator A_0^{-1} to (74), we obtain a set of linear algebraic equations of the second kind (SLAE-2) for the unknown coefficients $\{x_{m,n}^{(\chi)}\}_{n=-\infty}^{+\infty}$ in the form of an operator equation,

$$X = A^*X + B^*, \tag{76}$$

where $A* = A_0^{-1}A1$ and $B* = A_0^{-1}B$ have the norms, bounded in the space ℓ^2.

In particular, in the case of a single cone with one slot $(\theta_0 = \pi,\ N = 1)$, excited by the elementary radial electric dipole $(\chi = 1)$, the unknown coefficients $x_n^{(1)}$ are the solutions of the following SLAE-2:

$$x_0^{(1)}\left\{D_{i\tau}^{(1)}-\ln\frac{1-u}{2}\right\}+D_{i\tau}^{(1)}\sum_{p=1}^{+\infty}(-1)^p x_p^{(1)}\varepsilon_p^{(1)}\left[P_p(u)+P_{-p}(u)\right]=D_{i\tau}^{(1)}, \tag{77}$$

$$(-1)^n\frac{D_{i\tau}^{(1),n}}{D_{i\tau}^{(1)}}x_0^{(1)}\left[P_n(u)+P_{-n}(u)\right]+2D_{i\tau}^{(1),n}(-1)^{n+1}+\sum_{p=1}^{+\infty}(-1)^p p x_p^{(1)}\varepsilon_p^{(1)}\left[V_{n-1}^{p-1}(u)+V_{-n-1}^{p-1}(u)\right]-2x_n^{(1)}=0,\ n=1,2,..., \tag{78}$$

where $D_{i\tau}^{(1)}=D_{i\tau}^{(1)}(\gamma)=\frac{\pi}{\mathrm{ch}\pi\tau}P_{-1/2+i\tau}(\cos\gamma)P_{-1/2+i\tau}(-\cos\gamma)$,

$$D_{i\tau}^{(1),n}=D_{i\tau}^{(1),n}(\gamma)=(-1)^n\frac{\pi}{\mathrm{ch}\pi\tau}\frac{\Gamma(1/2+i\tau-n)}{\Gamma(1/2+i\tau+n)}P_{-1/2+i\tau}^{n}(\cos\gamma)P_{-1/2+i\tau}^{n}(-\cos\gamma), \tag{79}$$

$$N|n|\left(1-\varepsilon_n^{(1)}\right)=\frac{(-1)^{nN}\mathrm{ch}\pi\tau}{\pi\sin\gamma}\frac{\Gamma(1/2+i\tau+nN)}{\Gamma(1/2+i\tau-nN)}\frac{1}{P_{-1/2+i\tau}^{nN}(-\cos\gamma)P_{-1/2+i\tau}^{nN}(\cos\gamma)^{-1}}, \tag{80}$$

where $u=-\cos(d/2)$.

The absolute values of Fourier coefficients $x_0^{(1)}$, $x_1^{(1)}$ and $x_2^{(1)}$ of the electromagnetic field components versus slot width d are presented in Figure 2 for various values of integration parameter τ and aperture angle γ. It should be noted that in the case of the axially symmetric excitation of the isotropic zero-thickness PEC cone (i.e. in the absence of slots $d=0$), the Fourier coefficient is $x_0^{(1)}=1$ and $x_n^{(1)}=0$ for all $n\neq 0$.

The spatial spectrum of the initial-boundary problem is defined by the poles of the function $U_{0,\tilde{\mu}}^{(1)}(\theta,\varphi)$ (69). In this case, the spectrum of the initial-boundary problem $\{\tilde{\mu}_s\}_{s=0}^{+\infty}$ is defined by the poles of the $x_n^{(1)}$ coefficients,

$$x_n^{(1)}=\frac{\Delta_{\tilde{\mu},n}^{(1)}}{\Delta_{\tilde{\mu}}^{(1)}}, \tag{81}$$

where $\Delta_{i\tau}^{(1)}$ is the matrix determinant of the SLAE-2 (77), (78).

The plots in Figure 3 show the first three spectral values $\tilde{\mu}_n$, $n=0,1,2$ as a function of slot width d for different values of aperture angle γ.

Note that the values of the parameter $\alpha=-1/2+\tilde{\mu}_0^{(1)}$, $\tilde{\mu}_0^{(1)}=\min_s\tilde{\mu}_s^{(1)}$ define the electromagnetic field behaviour near the conical tip ($|\vec{E}|\sim r^{-1+\alpha}$, $|\vec{H}|\sim r^{\alpha}$, $r<<1$) and depend on

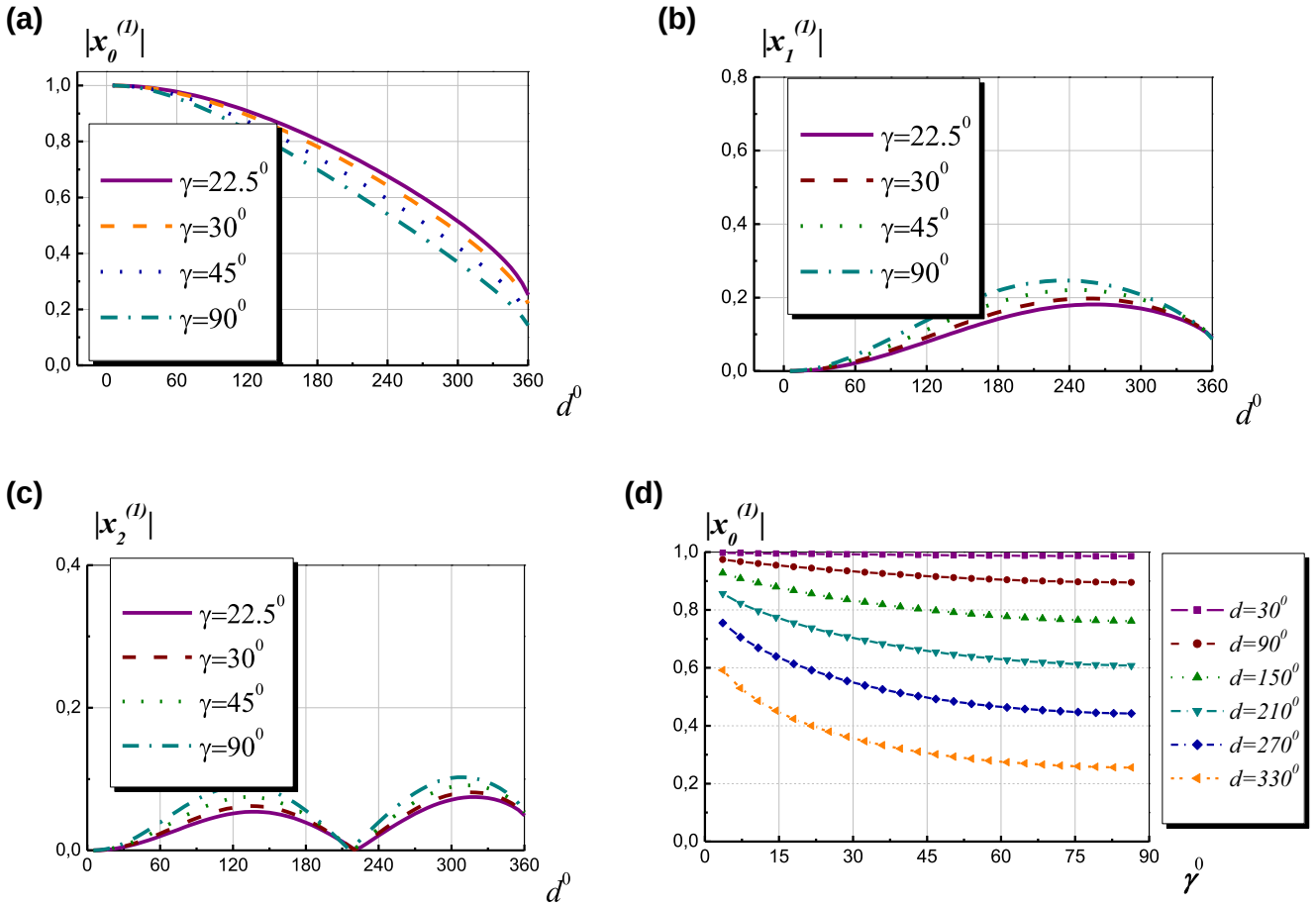

FIGURE 2 Dependences of the coefficients $|x_n^{(1)}|$ on the slot width d: (a) $n=0$, (b) $n=1$, (c) $n=2$; on the cone aperture angle γ: (d) $n=0$, $\tau=1$

its aperture angle γ and on slot width d. The dependences of parameter α on d are shown in Figure 4 for several values of γ.

Hence, finding the spectral values means solving the determinantal equation,

$$\Delta_{\tilde{\mu}}^{(1)}(d,\gamma,N)=0. \tag{82}$$

The electric field at the tip of a narrow isotropic cone ($\gamma << 1$) has significant singularity, while the magnetic field goes to zero. If the aperture angle increases, the electric field singularity at the tip of the isotropic cone decreases and progressively disappears if the cone turns into a plane (i.e. if $\gamma = \pi/2$).

A comparison of the field singularities for the isotropic cone and the cone with longitudinal slots, of the same aperture angle γ, shows that the presence of the slot makes the electric field singularity stronger. The magnetic field goes to zero at the cone tip, although the rate of decay is smaller than for the isotropic cone. If the slot is very wide, $d > 240^{\circ}$, aperture angle γ has little effect on the field singularity.

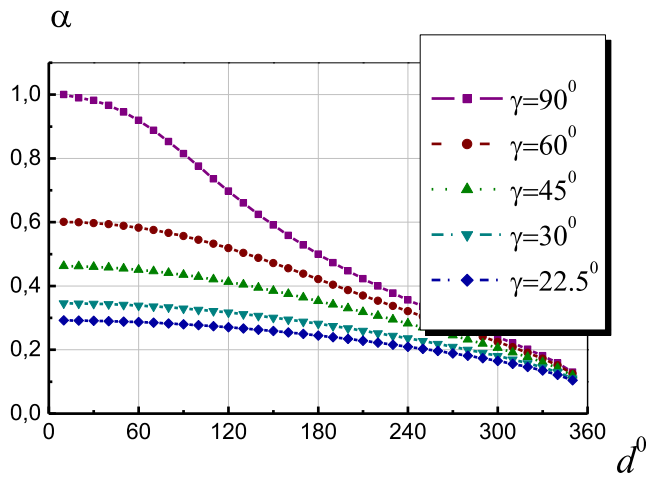

FIGURE 4 Parameter α as a function of slot width d for different cone aperture angle values, γ

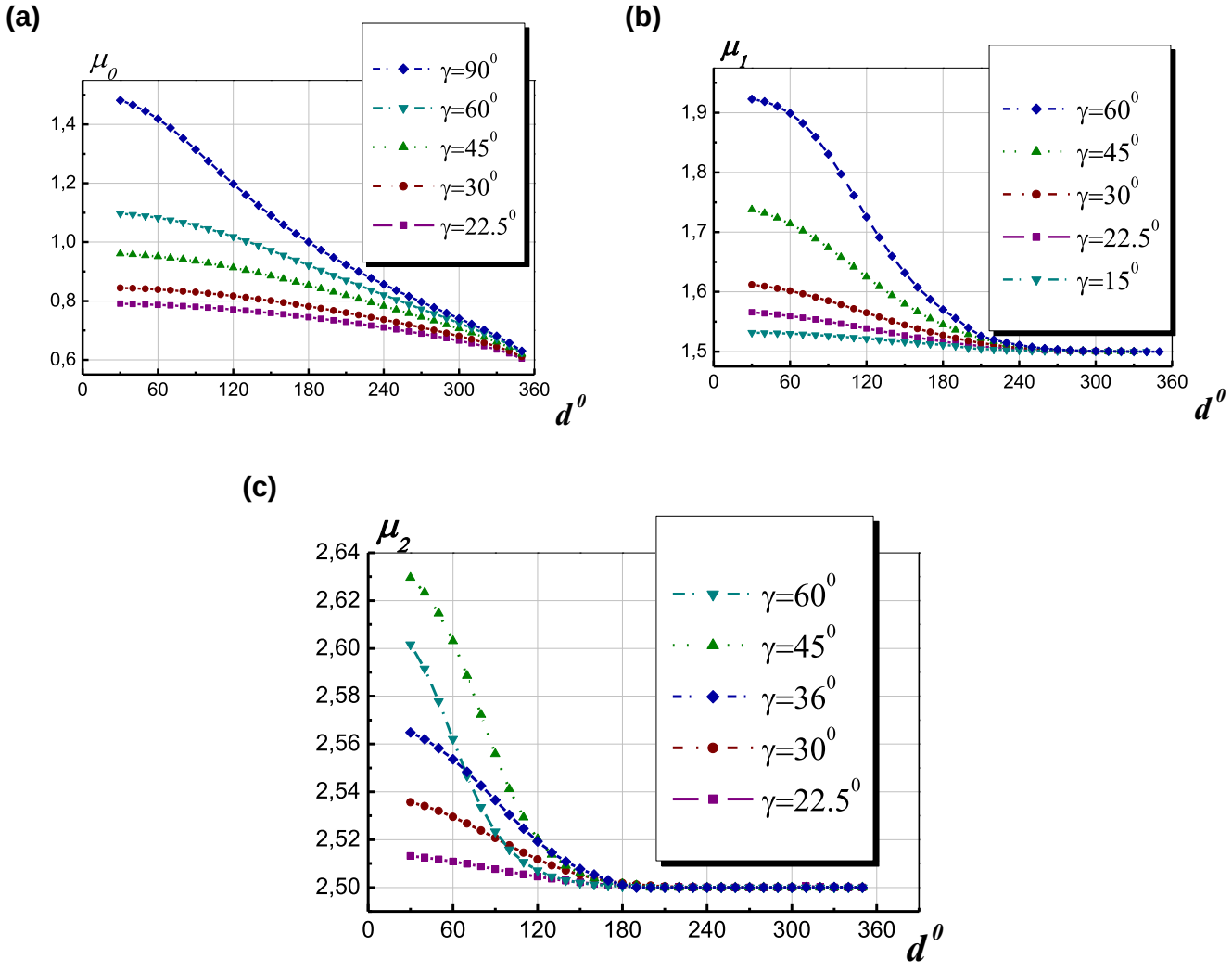

FIGURE 3 The dependencies of (a) $\tilde{\mu}_0$, (b) $\tilde{\mu}_1$, and (c) $\tilde{\mu}_2$ on slot width d for different values of aperture angle γ

In the case of the source location close to the cone tip ($r_0 << 1$),spectral value $\tilde{\mu}_0$ (Figure 3a defines the field amplitude.

5 | FIELDS PATTERNS. ANALYTICAL SOLUTIONS

In the case of the pulse excitation of a cone with one slot ($t_0 = 0, \chi = 2, \theta_0 = \pi, f(t) = \delta(t),\ N = 1$) (see Figure 5), the time-space dependence of the $H_{1\theta}$ field component is given by

$$H_{1,\theta}(\vec{r},t) = \frac{aM_r^{(\chi)}}{4\pi r r_0^{2}\varepsilon^{2-\chi}\mu^{\chi-1}}\eta\left(t-\frac{r+r_0}{a}\right)\sum_{n=-\infty}^{+\infty} e^{in\varphi} \times \int_0^{+\infty} \tau \mathrm{th}\pi\tau \hat{b}_{0\tau}^{(2)} \times \sum_{n=-\infty}^{+\infty} x_{0,n}^{(2)} \frac{\frac{d}{d\theta}P^{n}_{-1/2+i\tau}(-\cos\theta)}{\frac{d}{d\gamma}P^{n}_{-1/2+i\tau}(-\cos\gamma)} \frac{\partial}{\partial r} P_{-1/2+i\tau}[\mathrm{ch}b(t,r)]d\tau, \gamma < \theta < \pi. \tag{83}$$

The system of linear equations for the Fourier coefficients $x_{m,n}^{(2)}$ (further, $x_{m,n}^{(2)} = x_n^{(2)}$), in the case of the axially symmetric excitation of a single cone with one longitudinal slot Σ_2, has the following form:

$$x_0^{(2)}\left\{-\tilde{A}_{i\tau}^{(2),0} + \ln\frac{[1-u^{(2)}]}{2}\right\} + \sum_{p=1}^{+\infty} x_p^{(2)} \frac{\hat{\varepsilon}_p^{(2)}}{p}\left[P_p\left(u^{(2)}\right) + P_{-p}\left(u^{(2)}\right)\right] = \ln\frac{[1-u^{(2)}]}{2}, \tag{84}$$

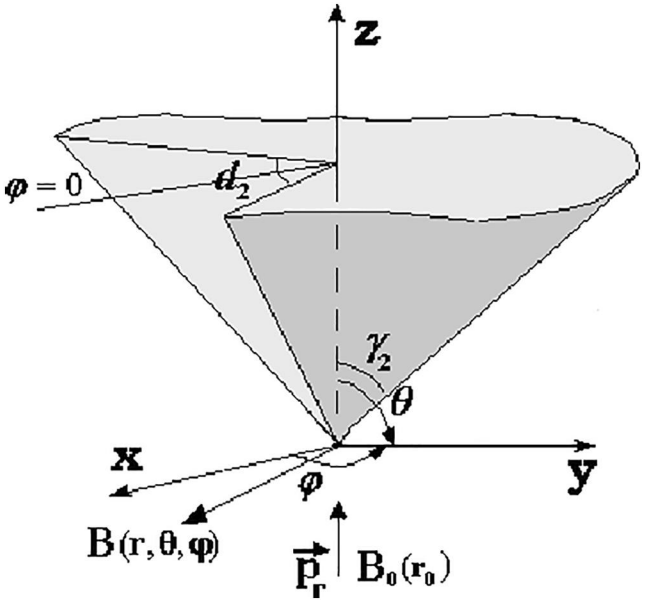

FIGURE 5 Cone with one longitudinal slot d_2, γ_2 is the cone aperture angle. The field source is located at point B_0 on the cone axis

$$x_0^{(2)}\left[P_n\left(u^{(2)}\right) + P_{-n}\left(u^{(2)}\right)\right] + 2\sum_{p=1}^{+\infty} x_p^{(2)}\hat{\varepsilon}_p^{(2)}\left[V_{n-1}^{p-1}\left(u^{(2)}\right) + V_{-n-1}^{p-1}\left(u^{(2)}\right)\right] - 2x_n^{(2)} = P_n\left(u^{(2)}\right) + P_{-n}\left(u^{(2)}\right), \quad n \neq 0. \tag{85}$$

As a criterion for the obtained solution convergence to the accurate solution (84), (85), the condition number can be used,

$$\nu_A = ||\grave{A}|| \cdot ||\grave{A}^{-1}||, \tag{86}$$

where $\breve{A}$ is the matrix of the $\breve{A}X = \breve{B}$ system. The condition number dependences for the SLAE-2 (84), (85) on slot width d_2 are given in Figure 6.

To illustrate the convergence speed, the relative truncation error of the SLAE-2 (84), (85) by the norm of the ℓ^2 space, can be used. Using the formula $X_L = \{x_n^{(2),L}\}$, this error can be defined as

$$e(L) = \frac{||X_L - X_{L+1}||_{l_2}}{||X_L||_{l_2}}. \tag{87}$$

Figure 7 illustrates the dependences of the relative truncation error on the truncation order L for four values of slot width d_2.

As is visible, a variation in slot width d_2 has no sizeable effect on the truncation error. In contrast, integration parameter τ is more important.

It can be seen in Figure 7 that it is enough to take 30 equations in the SLAE-2 (84), (85) if the integration parameter is $\tau = 20$, in order to obtain the solution with the relative error $e(L) \le 10^{-3}$.

The dependence of $H_{1\theta}$ on parameter $\xi = at/(r + r_0)$, $\xi > 1$ in the azimuth plane is given in Figure 8

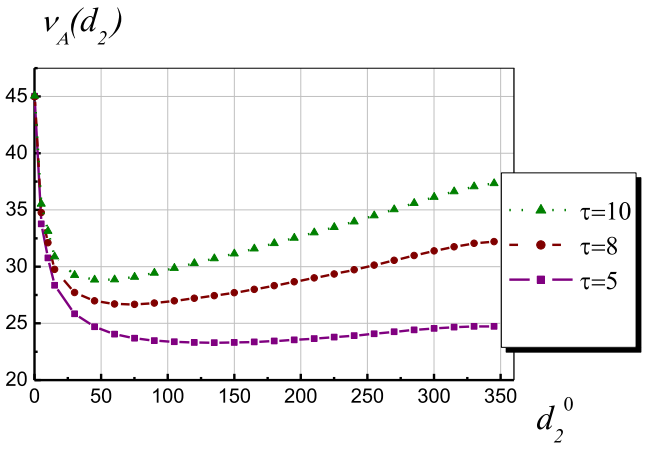

FIGURE 6 Condition number ν_A of the SLAE dependence on slot width d_2 for different values of integration parameter τ, $\gamma_2 = 22,5^0$

for fixed values of r, r_0, a, θ, γ, d and $\theta > 2\gamma$, $t > (r + r_0)/a$.

The minimum value, visible in the angular diagram, is explained by the slot effect because $\varphi = 0^0$ is the angular position of the slot centre.

The normalised far-field angular patterns in the azimuth plain that is orthogonal to the single-slot cone axis ($N = 1$, $\theta_0 = \pi, kr_0 = 1, \gamma_2 = .22.5^0, \theta = 60^0$) are shown in Figure 9. Note that the plain $\varphi = 0^0$ passes through the slot midpoint.

In the case of the time-harmonic excitation of a slotted PEC cone ($t_0 = 0$, $\chi = 2$, $\theta_0 = \pi$, $f(t) = e^{ia\omega t}$, $a = \pm 1$) (see Appendix B), we have

where $\Phi_{i\tau}(t, r) = \frac{2}{\pi a}\sqrt{rr_0}e^{ia\omega t}K_{i\tau}(qr_0)K_{i\tau}(qr)$, $K_{i\tau}(qr)$ is the McDonald function.

$$v_1^{(\chi)}(\overrightarrow{r}, t) = \frac{aM_r^{(\chi)}}{4\pi r r_0{}^2 \varepsilon^{2-\chi}\mu^{\chi-1}}\eta\left(t - t_0 - \frac{r + r_0}{a}\right) \times \sum_{m=-\infty}^{+\infty}(-1)^m e^{-im\varphi_0}\int_0^{+\infty}\tau \mathrm{th}\pi\tau\frac{\Gamma(1/2 - m + i\tau)}{\Gamma(1/2 + m + i\tau)}\hat{b}_{m\tau}^{(\chi)}U_{m,i\tau}^{(\chi)}(\theta, \varphi)\Phi_{i\tau}(t, r)d\tau, \quad (88)$$

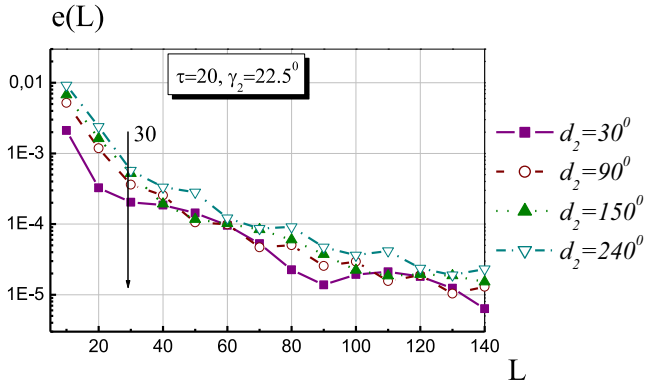

FIGURE 7 Relative error in the unknown coefficients $x_n^{(2)}$ versus the truncation order L of the SLAE-2 for different values of slot width d_2; the integration parameter is $\tau = 20$ and the cone angle is $\gamma_2 = \pi/8$

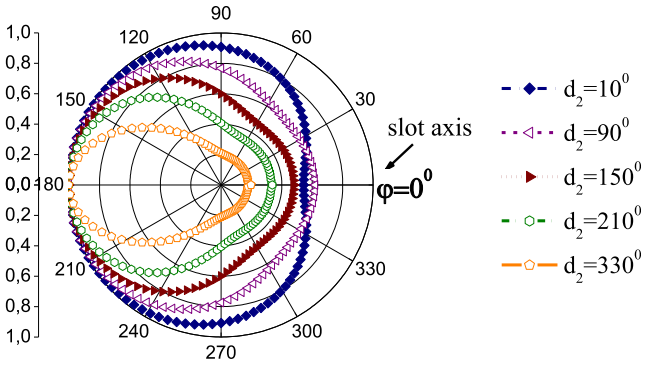

FIGURE 9 Diagrams of the normalised field distribution in the azimuth plain of the wave zone depending on slot width d_2 ($N = 1, \theta_0 = 180^0, kr_0 = 1, \gamma_2 = .22.5^0, \theta = 60^0$, ksi = 1.05)

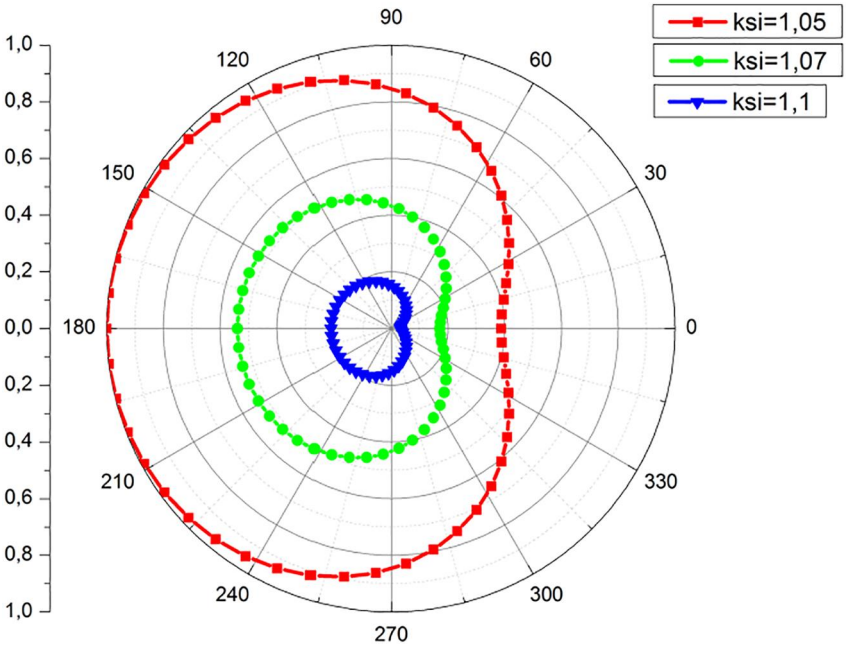

FIGURE 8 The dependence of $|H_{1\theta}|$ on the azimuth angle for various values of time parameter ξ; $r_0/r = 0.5$, $\gamma = \pi/8$, $d = \pi/6$

For the cone with N narrow slots, representation (88) is transformed (far from the slots) into the form ($\theta_0 = \pi$, $d_2/l << 1$, $(1-u^{(2)}) << 1$),

$$\upsilon_1^{(2),kn} = \upsilon_{1isotr.}^{(2)} - \frac{N}{\ln[\frac{1-u^{(2)}}{2}]} \int_0^\infty a_{i\tau}^{*(2)} \frac{K_{i\tau}(qr)}{\sqrt{r}} \times \frac{F_{i\tau}{}^*}{\Delta_{i\tau}^{(2),kn}} A_{i\tau}^{(2),0} P_{-1/2+i\tau}(-\cos\theta) d\tau + - \frac{N}{\ln[\frac{1-u^{(2)}}{2}]} \int_0^\infty a_{i\tau}^{*(2)} \frac{K_{i\tau}(qr)}{\sqrt{r}} \frac{F_{i\tau}^*}{\Delta_{i\tau}^{(2),kn}} A_{i\tau}^{(2),0} \times \sum_{n\neq 0} \frac{1}{1 - \frac{|n|}{n}\hat{\varepsilon}_{n,2}^{(2)} V_{n-1}^{n-1}(u_2)} \frac{P_{-1/2+i\tau}^{nN}(-\cos\theta)}{\frac{d}{d\gamma_2} P_{-1/2+i\tau}^{nN}(-\cos\gamma_2)} e^{inN\varphi} d\tau + O(1-u_2), \gamma_2 < \theta < \pi, \tag{89}$$

$$\Delta_{i\tau}^{(2),kn} = F_{i\tau}{}^* - \frac{1}{\ln[\frac{1-u^{(2)}}{2}]}, \quad F_{i\tau}{}^* = \frac{1}{A_{i\tau}^{(2),0} - N^{-1} \sum_{p\neq 0} |p|^{-1} \hat{\varepsilon}_{p,2}^{(2)}} \tag{90}$$

$$\Delta_{i\tau}^{(2),bcn} = \tilde{F}_{i\tau}{}^* - \frac{N}{\ln[\frac{1-u^{(2)}}{2}]} \tag{91}$$

$$a_{i\tau}^{*(2)} = \frac{\hat{p}_2}{2\pi^2 r_0} \tau th\pi\tau \frac{K_{i\tau}(qr_0)}{\sqrt{r_0}} \frac{\frac{d}{d\gamma_2} P_{-1/2+i\tau}(\cos\gamma_2)}{\frac{d}{d\gamma_2} P_{-1/2+i\tau}(-\cos\gamma_2)}, \quad \tilde{F}_{i\tau}{}^* = \frac{1}{\tilde{A}_{i\tau}^{*(2)} - \frac{1}{N} \sum_{p\neq 0} \frac{1}{|p|} \tilde{\varepsilon}_{p,2}^{(2)}}, \tag{92}$$

$$\tilde{A}_{i\tau}^{*(2)} = A_{i\tau}^{(2),0} \frac{1}{1 - \hat{C}_{i\tau}^{(2)}(\gamma_1, \gamma_2)}, u^{(2)} = \cos(\pi d_2/l), \tag{93}$$

$$A_{i\tau}^{(2),0} = -\frac{ch\pi\tau}{\pi \sin^2\gamma_2} \frac{1}{\frac{d}{d\gamma_2} P_{-1/2+i\tau}(\cos\gamma_2) \frac{d}{d\gamma_2} P_{-1/2+i\tau}(-\cos\gamma_2)} \tag{94}$$

The first term $\upsilon_{1isotr.}^{(2)}$ in the representation (90) corresponds to the Debye potential for the isotropic cone Σ_2 [31].

The spatial spectrum is the set of roots of the equations with small right-hand parts,

$$\frac{\pi \sin^2\gamma_2}{\cos\pi\tilde{\mu}} (\tilde{\mu}^2 - 1/4)^2 P_{-1/2+\tilde{\mu}}^{-1}(\cos\gamma_2) P_{-1/2+\tilde{\mu}}^{-1}(-\cos\gamma_2) = \frac{N}{\ln_2^1[1-u^{(2)}]}, \tag{95}$$

$$\frac{n \frac{d}{d\gamma_2} P_{-1/2+\tilde{\mu}}^{-nN}(\cos\gamma_2) \frac{d}{d\gamma_2} P_{-1/2+\tilde{\mu}}^{-nN}(-\cos\gamma_2)}{\frac{d}{d\gamma_2} P_{-1/2+\tilde{\mu}}^{-nN}(\cos\gamma_2) \frac{d}{d\gamma_2} P_{-1/2+\tilde{\mu}}^{-nN}(-\cos\gamma_2) + nN \frac{(-1)^{nN} \cos\pi\tilde{\mu}}{\pi \sin^2\gamma_2} \frac{\Gamma(1/2+\tilde{\mu}-nN)}{\Gamma(1/2+\tilde{\mu}+nN)}} = \frac{1}{2}(1-u^{(2)}). \tag{96}$$

All of those are located near the roots (see Appendix C) of equation $\frac{d}{d\gamma_2} P_{-1/2+\mu}(\pm\cos\gamma_2) = 0$, which corresponds to the case of the axially symmetric excitation of the isotropic PEC cone by the on-axis radial magnetic dipole ($\theta_0 = \pi$).

The expression for $\upsilon_{isotr.}^{(2)}$, corresponding to the full field, has the following form:

$$\upsilon_{isotr.}^{(2)} = \frac{b_{isotr.}^{(2)}}{\cos^2\frac{\gamma_2}{2}} \frac{\sin(kr_<)}{kr_0^2 r} e^{-ikr_>} + \frac{b_{isotr.}^{(2)*}}{r_0\sqrt{rr_0}} \sum_{n=1}^{+\infty} \frac{\alpha_n^{1-}}{\cos\pi\alpha_n^{1-}} J_{\alpha_n^{1-}}(kr_<) H_{\alpha_n^{1-}}^{(2)}(kr_>) \times \frac{P_{-1/2+\alpha_n^{1-}}^{-1}(\cos\gamma_2)}{\frac{d}{d\gamma} P_{-1/2+\tilde{\mu}}^{-1}(-\cos\gamma_2)\Big|_{\tilde{\mu}=\alpha_n^{1-}}} P_{-1/2+\alpha_n^{1-}}(-\cos\theta), \quad \gamma_2 < \theta < \pi, \tag{97}$$

$$\sin(kr_<) e^{-ikr_>} = \begin{cases} \sin kr e^{-ikr_0}, & r < r_0, \\ e^{-ikr} \sin kr_0, & r > r_0, \end{cases}$$

where $b_{isotr.}^{(2)}$ and $b_{isotr.}^{(2)*}$ are known coefficients. Corresponding to the $\tilde{\mu} = 1/2$ eigenvalue, which does not make any contribution to the field, the narrow slot's presence causes a perturbation in the spatial spectrum of the isotropic cone and the value $\tilde{\mu} = 1/2$ in particular. As a result, a guided wave corresponding to the ζ_1^{kn*} spectral value occurs in the scattering by the cone with a narrow slot field. The representation for one of the full-field components is provided below:

where

$$b_2^{\zeta_1^{kn*}}(\theta,\varphi) = c_1 + 2\frac{\sin\gamma_2}{\sin\theta} \frac{c_N(\cos N\varphi - c_N)}{1 - 2c_N\cos N\varphi + c_N^2},$$

where $c_N = \left(\frac{\cot\frac{\theta}{2}}{\cot\frac{\gamma_2}{2}}\right)^N$, $f_{\alpha_m^{1-}}^{*(-1)}$ are known functions.

$$H_{1\theta}=\frac{b^{(2)*}_{isotr.}}{rr_0\sqrt{r_0}}\sum_{m=1}^{+\infty}\left(\frac{kr_0}{2}\right)^{\tilde{\mu}^{1-}_m-\alpha^{1-}_m}\frac{\alpha^{1-}_m\left[\left(\alpha^{1-}_m\right)^2-1/4\right]}{\cos\pi\alpha^{1-}_m}J_{\alpha^{1-}_m}(kr_0)\frac{d}{dr}\left(\sqrt{r}H^{(2)}_{\alpha^{1-}_m}(kr)\right)$$
$$\times\left.\frac{P^{-1}_{-1/2+\tilde{\mu}}(\cos\gamma_2)}{\frac{d}{d\tilde{\mu}}P^{-1}_{-1/2+\tilde{\mu}}(-\cos\gamma_2)}\right|_{\tilde{\mu}=\alpha^{1-}_m}\cdot P^{-1}_{-1/2+\alpha^{1-}_m}(-\cos\theta)+\frac{b_{\zeta^{kn}_1}\tan\frac{\gamma_2}{2}}{2\sin^2\gamma_2\frac{N}{\ln\frac{1-u^{(2)}}{2}}}\left(\frac{kr_0}{2}\right)^{-3/2+\zeta^{kn}_1}\frac{\sin kr_0}{r_0}b^{\zeta^{kn}_1}_2(\theta,\varphi)\frac{e^{-ikr}}{r}$$
$$+\frac{1}{\sin^2\gamma_2\frac{1}{N}\ln\frac{1-u^{(2)}}{2}}\frac{b^{*(2)}_1}{rr_0\sqrt{r_0}}\left\{\sum_{m=1}^{+\infty}\left(\frac{kr_0}{2}\right)^{\tilde{\mu}^{1-}_m-\alpha^{1-}_m}\left.\frac{\tilde{\mu}J_{\tilde{\mu}}(kr_0)}{\left[\frac{d}{d\tilde{\mu}}P^{-1}_{-1/2+\tilde{\mu}}(-\cos\gamma_2)\right]^2}\right|_{\tilde{\mu}=\alpha^{1-}_m}\right.$$
$$\times\frac{d}{dr}\left[\sqrt{r}H^{(2)}_{\alpha^{1-}_m}(kr)\right]P^{-1}_{-1/2+\alpha^{1-}_m}(-\cos\theta)f^{*(-1)}_{\alpha^{1-}_m}$$
$$\left.+2\sum_{n=1}^{+\infty}\cos nN\varphi\sum_{m=1}^{+\infty}\left(\frac{kr_0}{2}\right)^{\tilde{\mu}^{1-}_m-\alpha^{1-}_m}\times J_{\alpha^{1-}_m}(kr_0)\left.\frac{\tilde{\mu}\frac{d}{dr}\left[\sqrt{r}H^{(2)}_{\tilde{\mu}}(kr)\right]}{\frac{d}{d\tilde{\mu}}P^{-1}_{-1/2+\tilde{\mu}}(-\cos\gamma_2)}\frac{\frac{d}{d\theta}P^{-nN}_{-1/2+\tilde{\mu}}(-\cos\theta)}{\frac{d}{d\gamma_2}P^{-nN}_{-1/2+\tilde{\mu}}(-\cos\gamma_2)}\right|_{\tilde{\mu}=\alpha^{1-}_m}\right\}$$
$$+O\left(\ln^{-2}\left(1-u^{(2)}\right)\right),r_0<r,\gamma_2<\theta<\pi, \tag{98}$$

The summand

$$\frac{b_{\zeta^{kn}_1}\tan\frac{\gamma_2}{2}}{2\sin^2\gamma_2\frac{1}{N}\ln\frac{1-u^{(2)}}{2}}\left(\frac{kr_0}{2}\right)^{-3/2+\zeta^{kn}_1}\frac{\sin kr_0}{r_0}b^{\zeta^{kn}_1}_2(\theta,\varphi)\frac{e^{-ikr}}{r}, \tag{99}$$

in formula (98) corresponds to ζ^{kn}_1 (see Appendix, C3). It represents the wave propagating from the cone apex for $r_0<r$ (the travelling slot wave) and the standing wave e (98), if $r<r_0$. The terms corresponding to the eigenvalues located near the roots of $\frac{d}{d\gamma_2}P^{-nN}_{-1/2+\tilde{\mu}}(\pm\cos\gamma_2)=0, nN\geq 1$ and $\frac{d}{d\gamma_2}P^{-1}_{-1/2+\tilde{\mu}}(\cos\gamma_2)=0$ have the order $O(\ln^{-2}(1-u^{(2)}))$ or higher; therefore, they are not present in the representations (98), since they are defined with the accuracy of this same order. Thus, the considered terms of decompositions (98) correspond to eigenvalues ζ^{kn}_1 and $\tilde{\tilde{\mu}}^{1-}_n$.

Provided that the structure is excited by the magnetic radial dipole, the magnetic field behaviour near the isotropic cone apex is characterised by the term $(kr)^{-3/2+\beta(\gamma)}$, where $\beta(\gamma)=\min\beta_n>3/2$. This means that in this case the field has no singularity near the apex. The slots cause a perturbation in the isotropic cone spatial spectrum; so the terms corresponding to the slots enter the result\ in addition to the term representing the scattering by the isotropic cone field. In this case, the disturbed eigenvalue $\mu=1/2$ contributes to the scattered field. As a result, a singularity of the order of $(kr)^{-3/2+\zeta^{ki*}_1}$ appears in the cone with a narrow slot apex.

6 | CONCLUSIONS

We have studied, in the full-wave formulation, the problem of time-domain elementary dipole excitation of a zero-thickness PEC slotted biconical structure. Our analytical-numerical method is based on using the Mehler–Fock integral transform in combination with the method of analytical regularisation. We have derived the representations of the Debye potentials and the field components in the form of the Melher–Fock integrals and the series, which are convenient for studying the field in the transition regions, near the wave front, and in the approximation of the dipole location close to the complex cone tip. It has been shown that the spatial spectrum of the considered initial-boundary value problem depends only on the geometric parameters of the open conical structure and the minimum spectral value determines the behaviour of the electromagnetic field near the corner point (the apex of the cone or the centre of a slotted conical surface). The effect of the longitudinal slots on the spatial spectrum and structure of the field has been studied.

As for the wave-physics effects, we have found that the singularity of the electromagnetic field at the tip of a PEC cone with a longitudinal slot can be stronger than that at the tip of a solid PEC cone. We have also found simple approximations for the components of the field scattered by the considered conical surface for the dipole location close to the complex cone tip and near the wave front. The electromagnetic field

patterns depending on the time and the distance to the observation point have been presented.

As noted in the introduction, such conical and biconical structures with longitudinal slots are broadband structures. We believe that the appearance of additional slots with different widths will expand the range of capabilities of the corresponding antenna even further. The study of the problems of excitation of such structures can be carried out using the approach proposed in the work. The computed radiation patterns provide sufficient information about the far field (sectors of the highest and the lowest radiation) and this can be used, in particular, when solving the problems of electromagnetic compatibility. In the case where the source is located close to the tip, the regime of waves travelling along the slots or conical sectors has been identified and is of practical interest. When a cone with a narrow longitudinal slot is excited by a radial magnetic dipole (current loop), a slot wave appears in the scattered field. Its field has a strong singularity and modifies the field behaviour at the apex relative to what is observed on a solid cone. Therefore, slotted cones can find their applications in the measuring probes of diagnostic and control devices. Besides, in the case where the source is located near the tip, it is the field of this wave that has the main contribution to the antenna far-field radiation pattern.

Additionally, as it is the PEC scatterers that display the strongest field singularities [37–40], the method presented here can be used to solve the problem of pulsed excitation of imperfectly conducting (impedance, resistive and thin-dielectric) cones and bicones with longitudinal slots, where the field singularities are the same or weaker.

We believe that these results can be useful in the electromagnetic design of wide-band conical and biconical antennas and near-field probes.

ORCID

Nadiia P. Stognii https://orcid.org/0000-0001-6470-0717

REFERENCES

1. Rumsey, V.H.: Frequency Independent Antennas. Academic. Press, New York (1966)
2. Maloney, J.G., Smith, G.S.: Optimization of a conical antenna for pulse radiation: an efficient design using resistive loading. IEEE Trans. Antennas Propag. 41(7), 940–947 (1993)
3. Janaswamy, R., Shaubert, D.H., Pozar, D.M.: Analysis of the transverse electromagnetic modes of linearly tapered slot antenna. Radio Sci. 21(5), 797–804 (1986)
4. Bernard, J.M., Lyalinov, M.A.: Electromagnetic scattering by a smooth convex impedance cone. J. Appl. Math. 69, 285–333 (2004)
5. Lodge, O.J.: Electric telegraphy. United States Pattents No. 609,154. (1898)
6. Carlslaw, H.S.: The scattering sound waves by a cone. Math. Ann. 75(1), 133–147 (1914)
7. Schelkunoff, S.A., Friis, H.T.: Antennas Theory and Practice, p. 640. Willey Publications, New York (1952)
8. Wanselow, R.D., Milligan, D.W.: Broadband slotted cone antenna. IEEE Trans. Antennas Propag. AP-14(2), 170–182 (1966)
9. Syed, A.: The diffraction of arbitrary electromagnetic field by a finite perfectly conducting cone. J. Natl. Sci. Math. 2(1), 85–114 (1981)
10. Kraus, L., Levine, L.: Diffraction by an elliptic cone. Commun. Pure Appl. Math. 14, 49–68 (1961)
11. Smedt, R.D., Van Bladel, J.G.: Field singularities at the tip of a metallic cone of arbitrary cross section. IEEE Trans. Antennas Propag. AP-34(7), 865–870 (1986)
12. Ramsdail, P.A.: Antennas for communications. IEEE Commun. Mag. 19(5), 28–36 (1981)
13. Vafiadis, E., Sahalos, J.N.: The electromagnetic field of a slotted elliptic cone. IEEE Trans. Antennas Propag. 38(11), 1894–1898 (1990)
14. Smyshlyaev, V.P.: The high-frequency diffraction of electromagnetic waves by cones of arbitrary cross-section. SIAM J. Appl. Math. 53, 670–688 (1993)
15. Hansen, Th. B.: Diffraction by a plane angular sector, a new derivation. IEEE Trans. Antennas Propag. AP-38(11), 1892–1894 (1990)
16. Shen, H.-M., King, R.W.P.: V-conical antenna. IEEE Trans. Antennas Propag. 36(11), 1519–1525 (1988)
17. Keller, J.B.: Backscattering from a finite cone. IRE Trans. Antennas Propag. 8(11), 175–182 (1960)
18. Wang, D.-S., Medgyesi-Mitschang, L.N.: Electromagnetic scattering from finite circular and elliptic cone. IEEE Trans. Antennas Propag. AP-33(5), 488–497 (1985)
19. Ufimtsev, P.Y.: Fundamentals of the Physical Theory of Diffraction. Wiley-IEEE Press (2014)
20. Gomez Martin, R., Rubio Bretones, A., Pantoia, M.F.: Radiation characteristics of thin-wire V-antennas exited by arbitrary time-depended currents. IEEE Trans. Antennas Propag. AP-33(12), 1877–1880 (2001)
21. Hertel, T.V., Smith, G.S.: The conical spiral antenna over the ground. IEEE Trans. Antennas Propag. 50(12), 1468–1675 (2002)
22. Hong, S., Borrison, S.L.: Short-pulse scattering by a cone – direct and invers. IEEE Trans. Antennas Propag. AP-16(1), 98–102 (1968)
23. Stockbroeckx, B., Vorst, A.V.: Electromagnetic modes in conical transmission lines with the application to the linearly tapered slot antenna. IEEE Trans. Antennas Propag. 48(3), 447–455 (2000)
24. Lee, S.: Mutual admittance of slots on a cone. Solution by ray technique. IEEE Trans. Antennas Propag. AP-26(6), 768–773 (1978)
25. Dong, Y.-F., et al.: Optical properties of bow-antenna type nanoantennas integrated onto a silicon waveguide platform. IEEE Photon. J. 11(5), 6603019–20 (2019)
26. Sammadar, S., Mokole, L.: Biconical antennas with unequal cone angles. IEEE Trans. Antennas Propag. AP-46(2), 181–193 (1998)
27. Hadidi, A., Hamid, M.: Eigenvalues of a dielectric-coated conducting cone. IEEE Trans. Antennas Propag. AP-35(3), 299–304 (1987)
28. Hansen, T.B.: Corner diffraction coefficients for the quarter plane. IEEE Trans. Antennas Propag. AP-39(7), 976–984 (1991)
29. Adachi, S.: A theoretical analysis of semi-infinite conical antennas. IRE Trans. AP-8(8), 535–547 (1960)
30. Bladel, J.V.: Fields singularities at the tip of a dielectric cone. IEEE Trans. Antennas Propag. AP-33(8), 893–895 (1985)
31. Felsen, L., Marcuvitz, N.: Radiation and Scattering of Waves, p. 888. Wiley-IEEE (1973)
32. Kontorovich, M.I., Lebedev, N.N.: About one method for solving several problems of diffraction theory and related areas. J. Techn. Phys. 8(10–11), 1192–1206 (1938)
33. Kuryliak, D.B., Nazarchuk, Z.T.: Analytical-Numerical Methods in the Theory of Wave Diffraction on Conical and Wedge-Shaped Surfaces. Naukova Dumka Publications, Kyiv (2006)
34. Siegel, K.M.: Far field scattering from bodies of revolution. Appl. Sci. Res. 7(B), 293–328 (1959)
35. Britt, C.L.: Solution of electromagnetic scattering problems using time domain techniques. IEEE Trans. Antennas Propag. 37, 1181–1192 (1989)
36. Wang, Z.H., et al.: A novel broadband coaxial probe to conical wire transition at THz frequency. Progr. Electromagn. Res. Lett. 16, 31–45 (2011)
37. Nosich, A.I.: The method of analytical regularization in wave-scattering and eigenvalue problems: foundations and review of solutions. IEEE Antennas Propag. Mag. 41(3), 34–49 (1999)
38. Fikioris, G.: A note on the method of analytical regularization. IEEE Antennas Propag. Ma. 43(2), 4–40 (2001)

39. Kuryliak, D.B., Nazarchuk, Z.T.: Development of the methods of analytical regularization in the theory of diffraction. Mater. Sci. 47(2), 160–176 (2011)
40. Nosich, A.I.: Method of analytical regularization in computational photonics. Radio Sci. 51(3), 1421–1430 (2016)
41. Kvach, N.V., Sologub, V.G.: On the scattering of an e polarized planar wave by a finite number of tapes located in one plane. Radio Eng. Electron. Phys. 27(10), 154–156 (1982)
42. Nosich, A.I., Okuno, Y., Shiraishi, T.: Scattering and absorption of E and H-polarized plane waves by a circularly curved resistive strip. Radio Sci. 31(6), 1733–1742 (1996)
43. Booker, S.M., et al.: Benchmark problems for transient and ultrawideband scattering by metallic targets. Electromagnetics. 23(2), 169–186 (2003)
44. Radchenko, V.V., Sauleau, R., Nosich, A.I.: Radiation and absorption of waves emitted by a radial dipole in the presence of a layered dielectric sphere with a spherical screen. IET Microw. Antennas Propag. 6(9), 1063–1069 (2012)
45. Vinogradova, E.: Electromagnetic plane wave scattering by arbitrary two-dimensional cavities: rigorous approach. Wave Motion. 70, 47–64 (2017)
46. Oguzer, T., Altintas, A., Nosich, A.I.: Focusing of THz waves with a microsize parabolic reflector made of graphene in the free space. J. Eur. Opt. Soc. 13, 16 (2017)
47. Lucido, M., Santomassimo, C., Panariello, G.: The method of analytical preconditioning in the analysis of the propagation in dielectric waveguides with wedges. J. Lightwave Technol. 36(14), 2925–2932 (2018)
48. An, H., Matsushima, A.: Electromagnetic wave scattering from an infinite periodic array of hollow conducting circular cylinders of finite length. Progr. Electromagn. Res. C. 91, 1–13 (2019)
49. Kuryliak, D., Nazarchuk, Z., Lysechko, V.: Acoustic plane wave scattering from a soft finite truncated cone in axial irradiation. Acta Acustica Unit. Acustica. 105(3), 475–483 (2019)
50. Saidoglu, N.Y., Nosich, A.I.: Method of analytical regularization in the analysis of axially symmetric excitation of imperfect circular disk antennas. Comput. Math. Appl. 79(10), 2872–2884 (2020)
51. Lucido, M., Schettino, F., Panariello, G.: Scattering from a thin resistive disk: a guaranteed fast convergence technique. IEEE Trans. Antennas Propag. 69(1), 387–396 (2021)
52. Yevtushenko, F.O., et al.: Electromagnetic characterization of tuneable graphene-strips-on-substrate metasurface over entire THz range: analytical regularization and natural-mode resonance interplay. IET Microw. Antennas Propag. 15 (2021). https://doi.org/10.1049/mia2.12158
53. Lucido, M., Balaban, M.V., Nosich, A.I.: Plane wave scattering from thin dielectric disk in free space: generalized boundary conditions, regularizing Galerkin technique and whispering-gallery mode resonances. IET Microwa. Antennas Propag. 15 (2021). https://doi.org/10.1049/mia2.12106
54. Semenova, E.K., Doroshenko, V.A.: Electromagnetic excitation of PEC slotted cones by elementary radial dipoles – a semi-inversion analysis. Trans. Antennas Propag. 56(7), 1976–1983 (2008)
55. Chan, K.-K., Felsen, L.: Transient and time-harmonic diffraction by a semi-infinite cone. IEEE Trans. Antennas Propag. 25(6), 802–806 (1977)
56. Mandal, B.N.: Note on an integral transform. Bull. Math. Soc. Sci. Math. Republik Socialist Roumanie. 63, 87–93 (1971)
57. Lebedev, N.N., Skalskaya, I.P.: Integral representations related to Mehler-Fock transformations. Differ. Equa. 22, 1050–1056 (1986)

How to cite this article: Doroshenko, V.O., Stognii, N.P.: Integral transforms and the regularisation method in the time-domain excitation of open PEC slotted cone scatterers. IET Microw. Antennas Propag. 15(10), 1360–1379 (2021). https://doi.org/10.1049/mia2.12176

APPENDIX A

In this appendix, the Debye's potential $v_0^{(\chi)}$ for the electric ($\chi = 1$) and magnetic ($\chi = 2$) radial dipoles with the moment

$$\vec{P}^{(\chi)}(\vec{r},t) = \vec{M}_r^{(\chi)}\vec{e}_r\delta\left(\vec{r}-\vec{r}_0\right)f(t-t_0) \tag{A.1}$$

and the current density

$$\vec{j}^{(\chi)}(\vec{r},t) = \left(j_r^{(\chi)},0,0\right) \tag{A.2}$$

are derived.

These potentials have to satisfy the wave equation,

$$\left(\Delta - \frac{1}{a^2}\frac{\partial^2}{\partial t^2}\right)v_0^{(\chi)}(\vec{r},t) = -\hat{F}^{(\chi)}(\vec{r},t), \tag{A.3}$$

$$\hat{F}^{(\chi)}(\vec{r},t) = \frac{1}{\varepsilon^{2-\chi}\mu^{\chi-1}r}M_r^{(\chi)}\delta\left(\vec{r}-\vec{r}_0\right)f(t-t_0), \tag{A.4}$$

where

$$\Delta\tilde{W} = \frac{1}{r^2}\frac{\partial}{\partial r}\left(r^2\frac{\partial\tilde{W}}{\partial r}\right) + \frac{1}{r^2\sin\theta}\frac{\partial}{\partial\theta}\left(\sin\theta\frac{\partial\tilde{W}}{\partial\theta}\right) + \frac{1}{r^2\sin^2\theta}\frac{\partial^2\tilde{W}}{\partial\varphi^2}. \tag{A.5}$$

The solution of the equation (A.1) is found by means of the Green's function,

$$G(\vec{r},\vec{r},t,t') = \frac{\delta(t-t'-|\vec{r}-\vec{r}|/a)}{4\pi|\vec{r}-\vec{r}|} \tag{A.6}$$

Then the integral representation for the solution of (A.3) appears as follows:

$$v_0^{(\chi)}(\vec{r},t) = -\int_{-\infty}^{+\infty}dt'\int_\Omega\hat{F}^{(\chi)}(\vec{r},t')G(\vec{r},\vec{r},t,t')d\vec{r} = -\frac{1}{4\pi}\int_{-\infty}^{+\infty}dt'\int_\Omega\hat{F}^{(\chi)}(\vec{r},t')\frac{\delta(t-t'-|\vec{r}-\vec{r}|/a)}{|\vec{r}-\vec{r}|}d\vec{r}. \tag{A.7}$$

The integration in (A.3) is made over the entire space Ω. Taking into account (A.4) and (A.7), we have

$$v_0^{(\chi)}(\vec{r},t) = -\frac{M_r^{(\chi)}}{4\pi r_0 \varepsilon^{2-\chi}\mu^{\chi-1}}\frac{1}{R}f\left(t-t_0-\frac{1}{a}R\right)\eta\left(t-t_0-\frac{1}{a}R\right), \tag{A.8}$$

where $R = |\vec{r} - \vec{r}_0|$.

APPENDIX B

In this appendix, we derive the representation for the Debye's potential $v_1^{(\chi)}(\vec{r})$, corresponding to the scattered field in the case of the open biconical structure shown in Figure 1 and excited by a harmonic source, in the stabilised regime, at $t - t_0 >> 1$. The integral representation for the Debye's potential of the non-stationary problem contains the time parameter in the following function:

$$\eta\left(t-t_0-\frac{r+r_0}{a}\right)\Phi_{i\tau}(t,r). \tag{B.1}$$

We transform $\Phi_{i\tau}(t,r)$ so that it becomes convenient to pass to the stabilised (i.e. large-time) regime. The following expression should be taken into account:

$$P_{-1/2+i\tau}(\mathrm{ch}\alpha) = \frac{\sqrt{2}}{\pi}\int_0^{\alpha}\frac{\cos xy}{\sqrt{\mathrm{ch}\alpha - \mathrm{ch}y}}dy \tag{B.2}$$

provided that $t_0 = 0$, we obtain that

$$\Phi_{i\tau}(t,r) = \frac{2\sqrt{rr_0}}{\pi a}e^{i\varsigma\omega t}\int_0^{t}\eta\left(z-\frac{r+r_0}{a}\right)e^{-i\varsigma\omega z}dz \int_0^{b(z)}\frac{\cos(i\tau y)}{\sqrt{z^2-\xi^2/a^2}}dy, \tag{B.3}$$

where

$$\xi = \sqrt{r^2 + r_0^2 + 2rr_0\mathrm{ch}y}. \tag{B.4}$$

After the integration order changes in (B.3), we obtain the following representation for $\Phi_{i\tau}(t,r)$:

$$\Phi_{i\tau}(t,r) = \frac{2\sqrt{rr_0}}{\pi a}e^{i\varsigma\omega t}\int_0^{b(t)}\cos(i\tau y)dy\int_{\xi/a}^{+\infty}\frac{\eta(t-z)e^{-i\varsigma\omega z}}{\sqrt{z^2-\xi^2/a^2}}dz. \tag{B.5}$$

As a result of the passing in (B.5) to the stabilised regime ($t >> 1$), we get

$$\Phi_{i\tau}(t,r) = \frac{2\sqrt{rr_0}}{\pi a}e^{i\varsigma\omega t}\int_0^{+\infty}\cos(i\tau y)dy\int_{\xi/a}^{+\infty}\frac{\eta(t-z)e^{-i\varsigma\omega z}}{\sqrt{z^2-\xi^2/a^2}}dz. \tag{B.6}$$

Taking into account the fact that

$$K_0(q\xi) = \int_{\xi/a}^{+\infty}\frac{e^{-qaz}}{\sqrt{z^2-\xi^2/a^2}}dz, \tag{B.7}$$

$$K_{i\tau}(qr_0)K_{i\tau}(qr) = \frac{1}{2}\int_0^{+\infty}K_0\left(q\sqrt{r^2+r_0^2+2rr_0\mathrm{ch}y}\right)e^{i\tau y}dy, \tag{B.8}$$

we obtain from (B.6) the representation for function $\Phi_{i\tau}(t,r)$ in the stabilised regime,

$$\Phi_{i\tau}(t,r) = \frac{2}{\pi a}\sqrt{rr_0}e^{i\varsigma\omega t}K_{i\tau}(qr_0)K_{i\tau}(qr), \tag{B.9}$$

where $K_{i\tau}(qr)$ is the McDonald function. Taking into account (B.9), one obtains representation (87).

APPENDIX C

The spatial spectrum is a set of roots of the equations with small right-hand parts as follows:

$$\frac{\pi\sin^2\gamma_2}{\cos\pi\tilde{\mu}}(\tilde{\mu}^2-1/4)^2P^{-1}_{-1/2+\tilde{\mu}}(\cos\gamma_2)P^{-1}_{-1/2+\tilde{\mu}}(-\cos\gamma_2) = \frac{N}{\ln\frac{1}{2}[1-u^{(2)}]}, \tag{C.1}$$

$$\frac{n\frac{d}{d\gamma_2}P^{-nN}_{-1/2+\tilde{\mu}}(\cos\gamma_2)\frac{d}{d\gamma_2}P^{-nN}_{-1/2+\tilde{\mu}}(-\cos\gamma_2)}{\frac{d}{d\gamma_2}P^{-nN}_{-1/2+\tilde{\mu}}(\cos\gamma_2)\frac{d}{d\gamma_2}P^{-nN}_{-1/2+\tilde{\mu}}(-\cos\gamma_2) + nN\frac{(-1)^{nN}\cos\pi\tilde{\mu}}{\pi\sin^2\gamma_2}\frac{\Gamma(1/2+\tilde{\mu}-nN)}{\Gamma(1/2+\tilde{\mu}+nN)}} = \frac{1}{2}(1-u^{(2)}). \tag{C.2}$$

The roots of equation (C.2) have the following form:

$$\tilde{\tilde{\mu}}_n^{1-} = \alpha_n^{1-} + \frac{1}{\sin^2\gamma_2 \ln\frac{1-u^{(2)}}{2}} \frac{\cos\pi\tilde{\mu}}{\pi\left(\tilde{\mu}^2 - 1\Big/4\right) P^{-1}_{-1/2+\tilde{\mu}}\left(\cos\gamma_2\right)\frac{d}{d\tilde{\mu}}P^{-1}_{-1/2+\tilde{\mu}}\left(-\cos\gamma_2\right)}\Bigg|_{\mu=\alpha_n^{1-}} + O\left(\ln^{-2}\left(1-u^{(2)}\right)\right), \quad (C.3)$$

$$\tilde{\tilde{\mu}}_n^{1+} = \alpha_n^{1+} + \frac{1}{\sin^2\gamma_2 \ln\frac{1-u^{(2)}}{2}} \frac{\cos\pi\tilde{\mu}}{\pi(\tilde{\mu}^2 - 1/4) P^{-1}_{-1/2+\tilde{\mu}}(-\cos\gamma_2)\frac{d}{d\tilde{\mu}}P^{-1}_{-1/2+\tilde{\mu}}(\cos\gamma_2)}\Bigg|_{\mu=\alpha_n^{1+}} + O\left(\ln^{-2}(1-u_2)\right), \quad (C.4)$$

$$\zeta_1^{kn} = \frac{1}{2} - \frac{N}{\sin^2\gamma_2 \ln\frac{1-u^{(2)}}{2}} + O\left[\ln^{-2}\left(1-u^{(2)}\right)\right], \quad (C.5)$$

$$P^{-1}_{-1/2+\alpha_n^{1+}}(\cos\gamma_2) = 0, P^{-1}_{-1/2+\alpha_n^{1-}}(-\cos\gamma_2) = 0. \quad (C.6)$$